

Analytical investigation of 1D Darcy-Forchheimer flow under local thermal nonequilibrium

S. Müller and M. Rom

*Institut für Geometrie und Praktische Mathematik, RWTH Aachen University,
Templergraben 55, 52062 Aachen, Germany*
rom@igpm.rwth-aachen.de, mueller@igpm.rwth-aachen.de

Abstract

In the context of transpiration cooling, a 1D porous medium model consisting of a temperature system and a mass-momentum system is derived from the 2D/3D Darcy-Forchheimer equations. The temperatures of the coolant and the solid are assumed to be in local nonequilibrium. This system is analytically verified to have a unique solution. Transpiration cooling simulations are performed by a two-domain approach, coupling the assembled 1D porous medium solutions with 2D solutions of a hot gas flow solver. A comparison of results obtained by applying the 1D porous medium model with the temperature system either including or neglecting fluid heat conduction justifies the use of the latter simplified system.

Keywords: transpiration cooling, 1D porous medium flow, Darcy-Forchheimer, local thermal nonequilibrium

1 Introduction

Transpiration cooling is considered a promising heat protection technique for high-temperature and high-velocity gas flows. Compared with other active methods such as film cooling, it provides a superior cooling efficiency [1, 2]. A generic configuration is sketched in Fig. 1, where a cooling gas, initially stored in a reservoir, is driven through a porous medium such that it is injected into the hot gas flow. This is done by establishing a pressure difference between the hot gas and the coolant side.

In our former works [3–6], we present a two-domain approach for the numerical simulation of transpiration cooling problems, where a turbulent hot gas flow, e.g., a channel or a nozzle flow, is coupled with a laminar porous medium flow. For this purpose, we developed an iterative coupled procedure solving alternately the Reynolds-averaged Navier-Stokes equations in the hot gas domain and a system for mass, momentum and energy conservation in the porous medium domain. Momentum conservation is modeled by the Darcy-Forchheimer equation, and energy conservation is described by two temperature equations to account for a potential local thermal nonequilibrium between fluid and solid phase. For this coupled procedure, we developed appropriate coupling conditions, imposed at Γ_{Int} , see Fig. 1.

Using this two-domain approach, a wide variety of 2D and 3D test cases was investigated for different ranges of applications, cf. [3–8]. Although we found good agreement with experimental data, there are some numerical issues with respect to solving the porous medium flow. In particular, these concern the numerical stability of the solution method, especially in 3D, and the correct application of boundary conditions at the coolant reservoir and at the interface. Both problems contribute to an increase of the computation time. To overcome these issues and to generally accelerate computations, we recently developed in [9] a new coupled 2D/3D hot gas – assembled-1D porous medium flow solver, where the 2D or 3D hot gas flow is coupled to a porous medium which is decomposed into several 1D problems. These 1D problems are solved independently of each other and afterwards assembled to obtain a 2D or 3D solution for the porous medium flow. We refer to this coupled model as *assembled-1D model* in the following. In 1D, the *temperature system* (equations for fluid and solid temperature) can be decoupled

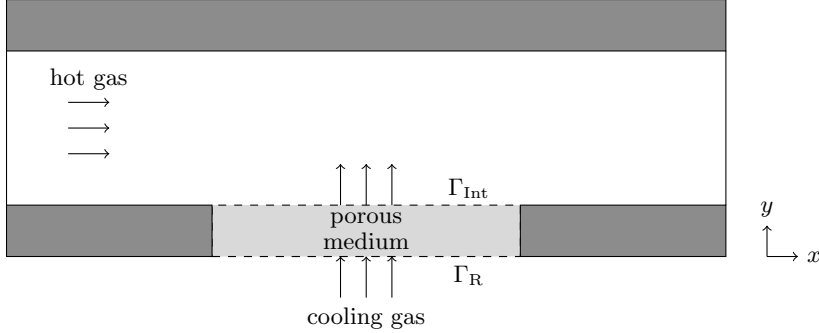


Figure 1: Illustration of 2D transpiration cooling setup (Γ_{R} : reservoir boundary, Γ_{Int} : interface between hot gas and porous medium).

from the *mass-momentum system* (continuity and Darcy-Forchheimer momentum equation) and solved analytically. The mass-momentum system can be rewritten making use of conservation of mass to obtain an ordinary differential equation for the density (or the velocity). From the numerical solution of the latter, the velocity (or the density) can be directly evaluated.

In [9], a 1D porous medium model is derived from a 2D/3D porous medium model. In contrast to previous work in the literature, where analytical solutions of the energy transport in 1D were in particular used to investigate the effect of different boundary conditions [10–13] or to predict wall temperatures in combination with a near-wall layer analysis of the hot gas flow [14–16], we impose other boundary conditions for the coupling with the hot gas flow. Furthermore, the mass-momentum system is included in the solvability analysis in [9] and in the current work.

For the assembled-1D model in [9], we use a simplified 1D porous medium temperature system. This is derived from the 2D/3D porous medium model used in our works [3–6] or works by other authors [17, 18] by neglecting effects due to fluid heat conduction. The simplification is based on the assumption that the thermal conductivity of the fluid in the porous medium is much smaller than the thermal conductivity of the solid phase. The main objective of the current work is the justification of this simplification. For this purpose, we first recall the 1D model in Sect. 2 composed of the temperature system with fluid heat conduction and the mass-momentum system. In Sect. 3, we determine the exact analytical solution of the temperature system. This enters the mass-momentum system that is verified to have a unique solution, see Sect. 4. By means of coupled simulations with the assembled-1D model using either the 1D temperature system with fluid heat conduction or the simplified one without, we verify in Sect. 5 that using the latter as in [9] will provide accurate results for the range of parameters in our transpiration cooling configuration.

2 One-dimensional model for porous medium flow in the context of transpiration cooling

In the following, we present the governing equations and boundary conditions for 1D stationary porous medium flow in local thermal nonequilibrium. The particular boundary conditions at the outlet of the porous medium establish the coupling with a hot gas flow for the simulation of transpiration cooling problems. More details on our original coupled two-domain approach can be found in [3–6]. The derivation of the 1D porous medium model and of the whole coupled assembled-1D model for transpiration cooling are presented in [9].

Governing equations. With ρ_f , v , \dot{m}_c and A_c denoting the fluid density, Darcy velocity, prescribed coolant mass flow rate and cross-sectional area of the porous probe, respectively, the one-dimensional model is obtained taking advantage of

$$\rho_f(y) v(y) = \frac{\dot{m}_c}{A_c} \quad (1)$$

being constant due to conservation of mass. Then, the 1D system of equations for $y \in (0, L)$, where L is

the length of the porous probe, splits into a system for mass and momentum

$$\rho'_f(y) v(y) + \rho_f(y) v'(y) = 0, \quad (2a)$$

$$\varphi^{-2} \rho_f(y) v(y) v'(y) = -R (\rho'_f(y) T_f(y) + \rho_f(y) T'_f(y)) - \frac{\mu_f}{K_D} v(y) - \frac{\rho_f(y)}{K_F} v(y)^2, \quad (2b)$$

and a temperature system

$$-\varphi \kappa_f T''_f(y) + c_{p,f} \frac{\dot{m}_c}{A_c} T'_f(y) = h_v (T_s(y) - T_f(y)), \quad (3a)$$

$$(1 - \varphi) \kappa_s T''_s(y) = h_v (T_s(y) - T_f(y)). \quad (3b)$$

The unknowns are fluid density ρ_f , Darcy velocity v , fluid temperature T_f and solid temperature T_s . All other quantities are given constant parameters, namely porosity φ of the porous probe, specific gas constant R , dynamic viscosity μ_f of the fluid, permeability K_D , Forchheimer coefficient K_F , specific heat capacity $c_{p,f}$ of the fluid, coolant mass flow rate \dot{m}_c , cross-sectional area A_c of the porous probe, volumetric heat transfer coefficient h_v , thermal conductivity κ_f of the fluid and thermal conductivity κ_s of the solid. Note that K_D , K_F and κ_s are scalars in 1D and matrices in 2D/3D. Consequently, only the respective values in flow direction y of those matrices are used in 1D. In (2b), we make use of the equation of state for an ideal gas $p(y) = \rho_f(y) R T_f(y)$, where p denotes the pressure. In 1D, the temperature system (3) can be solved independently from the mass-momentum system (2).

Boundary conditions. In 1D, boundary conditions have to be imposed only on the reservoir Γ_R and on the interface Γ_{Int} because the side walls of the porous medium do not exist. However, in [9] we show how the side walls can still be modeled for assembling a 2D or 3D porous medium solution from the individual 1D solutions.

- On the reservoir Γ_R at $y = 0$:

$$T_f(0) = T_b, \quad (4a)$$

$$T_s(0) = T_b, \quad (4b)$$

where T_b is the constant backside temperature of the porous probe.

- On the interface Γ_{Int} at $y = L$:

$$\rho_f(L) = \frac{p_{\text{HG}}}{R T_f(L)}, \quad (5a)$$

$$v(L) = \frac{\dot{m}_c}{A_c} \frac{R T_f(L)}{p_{\text{HG}}}, \quad (5b)$$

$$(1 - \varphi) \kappa_s T'_s(L) = q_{\text{HG}} - c_{p,f} \frac{\dot{m}_c}{A_c} (T_s(L) - T_f(L)), \quad (5c)$$

$$T'_f(L) = \frac{h_v A_c}{c_{p,f} \dot{m}_c} (T_s(L) - T_f(L)). \quad (5d)$$

Here, p_{HG} and $q_{\text{HG}} = \kappa_{\text{HG}} T'_{\text{HG}}$ are the pressure and the heat flux, respectively, in the hot gas at the interface. For each 1D porous medium problem, both p_{HG} and q_{HG} are constant values such that the coordinate dependence of the hot gas values is omitted.

The boundary condition (5d) for $T'_f(L)$ is based on the simplification of the equation for the fluid temperature (3a). It is obtained by setting $y = L$ and neglecting the first term on the left-hand side, i.e., $-\varphi \kappa_f T''_f(y)$. This is a common simplification for cases in which $\kappa_f \ll \kappa_s$ such as transpiration cooling problems, see for instance [11, 19]. Other works such as [18] use $T'_f(L) = 0$ instead, assuming that the convective heat flux from the hot gas side is fully absorbed by the solid in the porous medium. However, despite imposing $T'_f(L) = 0$ an adiabatic behavior of the fluid temperature at the interface is usually not observable in simulations where $\kappa_f \ll \kappa_s$. This is due to the strong coupling of the two temperature equations and fluid heat conduction being negligible. The influence of the different boundary conditions for $T'_f(L)$ is investigated in Sect. 5.

Solution procedure. The resulting 1D porous medium model becomes a boundary value problem. Its solution requires to solve three subproblems for the temperatures T_f and T_s , the density ρ_f and the velocity v , respectively. First of all, we solve the temperature system (3) with boundary conditions (4a), (4b) at $y = 0$ as well as (5c), (5d) at $y = L$. Since these problems are linear, we can solve them explicitly.

The temperature solution enters the initial value problem (2a) for the density with initial condition (5a) at $y = L$ as parameter. Under some assumptions, its solution can be verified to exist but is not known explicitly because the initial value problem is nonlinear. Instead, it will be approximated numerically applying some ODE solver. This is done by treating (2a) as a backward problem using the boundary condition for $\rho_f(L)$ given in (5a) and employing mass conservation (1).

Finally, we may determine algebraically the solution of the velocity employing constant mass flow (1). In particular, (5b) holds at $y = L$. Note that due to mass conservation we alternatively may first solve the velocity and then determine the density.

Remark 1 (Simplified temperature model). *As discussed above, if $\kappa_f \ll \kappa_s$, fluid heat conduction is negligible and the resulting simplified temperature system as used for our assembled-1D model in [9] is given by*

$$c_{p,f} \frac{\dot{m}_c}{A_c} T_f'(y) = h_v (T_s(y) - T_f(y)), \quad (6a)$$

$$(1 - \varphi) \kappa_s T_s''(y) = h_v (T_s(y) - T_f(y)), \quad (6b)$$

omitting the term $-\varphi \kappa_f T_f''(y)$ in (6a). Due to neglecting fluid heat conduction effects and, hence, the second-order derivative of the fluid temperature T_f , the boundary condition (5d) for $T_f'(L)$ is not needed for the simplified temperature model.

In Sects. 3 and 4, we show under which assumptions the equations for the two temperatures including the term $-\varphi \kappa_f T_f''(y)$ and the one for the density have unique solutions. These assumptions ensure monotonicity of the temperatures, the density and the velocity.

3 Temperature system with fluid heat conduction

For the investigation of the temperature system determined by (3) and corresponding boundary conditions (4a), (4b) at $y = 0$ and (5c), (5d) at $y = L$, we rewrite the model in a more canonical form. For this purpose, we introduce the derivatives of the temperatures as additional unknowns, i.e., $T_{f,1} := T_f$, $T_{f,2} := T_f'$, $T_{s,1} := T_s$, $T_{s,2} := T_s'$:

$$T_{f,1}'(y) = T_{f,2}(y), \quad (7a)$$

$$T_{f,2}'(y) = -\frac{1}{\varphi \kappa_f} \left(h_v (T_{s,1}(y) - T_{f,1}(y)) - c_{p,f} \frac{\dot{m}_c}{A_c} T_{f,2}(y) \right), \quad (7b)$$

$$T_{s,1}'(y) = T_{s,2}(y), \quad (7c)$$

$$T_{s,2}'(y) = \frac{1}{(1 - \varphi) \kappa_s} h_v (T_{s,1}(y) - T_{f,1}(y)) \quad (7d)$$

for $y \in (0, L)$ with boundary conditions

$$T_{f,1}(0) = T_b, \quad T_{s,1}(0) = T_b, \quad (8a)$$

$$T_{f,2}(L) = \frac{h_v A_c}{c_{p,f} \dot{m}_c} (T_{s,1}(L) - T_{f,1}(L)), \quad (8b)$$

$$T_{s,2}(L) = \frac{1}{(1 - \varphi) \kappa_s} \left(c_{p,f} \frac{\dot{m}_c}{A_c} (T_{f,1}(L) - T_{s,1}(L)) + q_{HG} \right).$$

We solve this boundary value problem by means of a shooting procedure where in a first step we solve the linear homogeneous first order initial value problem

$$\mathbf{z}'(y) = \mathbf{A}\mathbf{z}(y), \quad y \in (0, L) \quad (9)$$

with

$$\mathbf{A} := \begin{pmatrix} 0 & 1 & 0 & 0 \\ a & b & -a & 0 \\ 0 & 0 & 0 & 1 \\ -c & 0 & c & 0 \end{pmatrix}, \quad \mathbf{z} := \begin{pmatrix} T_{f,1} \\ T_{f,2} \\ T_{s,1} \\ T_{s,2} \end{pmatrix}, \quad (10)$$

positive matrix entries

$$a := \frac{h_v}{\varphi \kappa_f}, \quad b := \frac{c_{p,f} \dot{m}_c}{A_c \varphi \kappa_f}, \quad c := \frac{h_v}{(1-\varphi) \kappa_s} \quad (11)$$

and initial conditions

$$\mathbf{z}(0) = (T_f(0), s_1, T_s(0), s_2)^T = (T_b, s_1, T_b, s_2)^T \equiv \mathbf{z}(0; s_1, s_2). \quad (12)$$

Then the shooting parameters (s_1, s_2) are determined such that the solution of the initial value problem $\mathbf{z} = \mathbf{z}(\cdot; s_1, s_2)$ satisfies the boundary conditions

$$z_2(L; s_1, s_2) = \alpha (z_3(L; s_1, s_2) - z_1(L; s_1, s_2)), \quad (13a)$$

$$z_4(L; s_1, s_2) = \beta (z_1(L; s_1, s_2) - z_3(L; s_1, s_2)) + \gamma \quad (13b)$$

with

$$\alpha := \frac{h_v A_c}{c_{p,f} \dot{m}_c} = \frac{a}{b}, \quad \beta := \frac{1}{(1-\varphi) \kappa_s} \frac{c_{p,f} \dot{m}_c}{A_c} = \frac{cb}{a}, \quad (14a)$$

$$\gamma := \frac{1}{(1-\varphi) \kappa_s} q_{\text{HG}}. \quad (14b)$$

To determine the unique solution of the parameter-dependent initial value problem, we determine the eigenvalues and eigenvectors of the matrix \mathbf{A} . The characteristic polynomial is

$$\det(\mathbf{A} - \lambda \mathbf{I}) = \lambda p_3(\lambda) \quad \text{with} \quad p_3(\lambda) = \lambda^3 - b\lambda^2 - (a+c)\lambda + cb. \quad (15)$$

First of all, we investigate the roots of the cubic polynomial p_3 .

Proposition 1 (Properties of cubic polynomial).

There exist three real roots λ_k , $k = 0, 1, 2$, of the polynomial p_3 with the following properties:

(i) *the roots are explicitly given by*

$$\lambda_k = 2\sqrt{\frac{3(a+c) + b^2}{9}} \cos\left(\frac{\theta}{3} + \frac{2k\pi}{3}\right) + \frac{b}{3}, \quad (16)$$

$$\cos \theta = \frac{b}{2} \frac{2b^2 + 9(a+c) - 27c}{(3(a+c) + b^2)^{3/2}};$$

(ii) *the roots can be estimated by*

$$\lambda_0 \in (\max(b, \sqrt{c}), +\infty), \quad \lambda_1 \in (-\infty, -\sqrt{c}), \quad \lambda_2 \in (0, \min(b, \sqrt{c})); \quad (17)$$

(iii) *the roots satisfy the relations*

$$b = \lambda_0 + \lambda_1 + \lambda_2, \quad a + c = -(\lambda_1 \lambda_2 + \lambda_0 \lambda_1 + \lambda_0 \lambda_2), \quad cb = -\lambda_0 \lambda_1 \lambda_2; \quad (18)$$

(iv) *the following estimates hold:*

$$c - \lambda_0^2 < 0, \quad c - \lambda_1^2 < 0, \quad c - \lambda_2^2 > 0, \quad (19a)$$

$$\lambda_2 < |\lambda_1| < \lambda_0. \quad (19b)$$

Proof. First of all, we check the existence of the three distinct real roots. For this purpose, we observe that the polynomial changes its sign in three disjoint intervals:

$$\begin{aligned} p_3(-\infty) &= -\infty, \quad p_3(-\sqrt{c}) = a\sqrt{c} > 0, \\ p_3(0) &= cb > 0, \quad p_3(\sqrt{c}) = -a\sqrt{c} < 0, \\ p_3(b) &= -ab < 0, \quad p_3(+\infty) = +\infty. \end{aligned} \tag{20}$$

By continuity of the polynomial and the fundamental theorem of linear algebra, we conclude that there exist three distinct real roots in each of the intervals according to (17). These roots can be determined by Cardano's formula

$$\lambda_k = 2\varrho^{1/3} \cos\left(\frac{\theta}{3} + \frac{2k\pi}{3}\right) - \frac{r}{3}, \quad \varrho = \sqrt{-\frac{p^3}{27}}, \quad \cos\theta = -\frac{q}{2\varrho}, \quad k = 0, 1, 2$$

with

$$p = \frac{3s - r^2}{3}, \quad q = \frac{2r^3}{27} - \frac{rs}{3} + t, \quad r = -b, \quad s = -(a+c), \quad t = cb.$$

In terms of our coefficients, these are given by (16). To determine the corresponding sign of the roots, we note that by definition the angle $\theta \in [0, \pi]$. This implies for the angles $\theta_k := (\theta + 2k\pi)/3 \in [2k, 2k+1]\pi/3$ and, thus, $\theta_0 \in [0, \pi/3]$, $\theta_1 \in [2\pi/3, \pi]$ and $\theta_2 \in [4\pi/3, 5\pi/3]$. For the cosine factors, we conclude $\cos(\theta_0) \in [0.5, 1]$, $\cos(\theta_1) \in [-1, -0.5]$ and $\cos(\theta_2) \in [-0.5, 0.5]$. This corresponds to (17).

By the fundamental theorem of algebra, it holds $p_3(\lambda) = (\lambda - \lambda_0)(\lambda - \lambda_1)(\lambda - \lambda_2)$. By comparison of coefficients, the relations (18) must hold.

The estimate (19a) follows by (17). For the estimate (19b), we conclude from $\lambda_0 + \lambda_1 + \lambda_2 = b$ and $\lambda_0 > b$ that $\lambda_1 + \lambda_2 < 0$ holds. Because of $\lambda_1 < 0$ and $\lambda_2 > 0$, this implies $\lambda_2 < |\lambda_1|$ and, thus, $\lambda_0 + \lambda_1 > 0$. \square

Remark 2 (Estimate of the roots).

Note that the estimate $\lambda_0 > b$ is stronger than $\lambda_0 > \sqrt{c}$ because b is independent of h_v . Therefore, the root λ_0 is always large due to physical reasons. Then we may neglect terms $e^{-\lambda_0 L}$ later on.

The fourth eigenvalue is $\lambda_3 = 0$ that is distinct to the others. Thus, there exist four linearly independent eigenvectors

$$\mathbf{v}_k = c^{-1} (c - \lambda_k^2, (c - \lambda_k^2)\lambda_k, c, c\lambda_k)^T, \quad k = 0, 1, 2, \quad \mathbf{v}_3 = (1, 0, 1, 0)^T.$$

Then the unique solution of the parameter-dependent initial value problem is determined by

$$\mathbf{z}(y; s_1, s_2) = \mathbf{W}(y)\mathbf{W}(0)^{-1}\mathbf{z}(0; s_1, s_2) = \mathbf{V}\mathbf{D}(y)\mathbf{V}^{-1}\mathbf{z}(0; s_1, s_2) \tag{21}$$

with Wronski matrix

$$\mathbf{W}(y) = \mathbf{V}\mathbf{D}(y), \quad \mathbf{V} := (\mathbf{v}_0, \mathbf{v}_1, \mathbf{v}_2, \mathbf{v}_3), \quad \mathbf{D}(y) := \text{diag}(e^{\lambda_0 y}, e^{\lambda_1 y}, e^{\lambda_2 y}, e^{\lambda_3 y}). \tag{22}$$

Here, \mathbf{V} denotes the matrix of right eigenvectors of the matrix \mathbf{A}

$$\mathbf{V} = \begin{pmatrix} \frac{c-\lambda_0^2}{c} & \frac{c-\lambda_1^2}{c} & \frac{c-\lambda_2^2}{c} & 1 \\ \frac{(c-\lambda_0^2)\lambda_0}{c} & \frac{(c-\lambda_1^2)\lambda_1}{c} & \frac{(c-\lambda_2^2)\lambda_2}{c} & 0 \\ 1 & 1 & 1 & 1 \\ \lambda_0 & \lambda_1 & \lambda_2 & 0 \end{pmatrix}$$

with its inverse determined by

$$\mathbf{V}^{-1} = \begin{pmatrix} \sigma_0 & 0 & 0 & 0 \\ 0 & \sigma_1 & 0 & 0 \\ 0 & 0 & \sigma_2 & 0 \\ 0 & 0 & 0 & \sigma_3 \end{pmatrix} \times \begin{pmatrix} -(b-\lambda_0) & 1 & b-\lambda_0 & \frac{b-\lambda_0}{\lambda_0} \\ b-\lambda_1 & -1 & -(b-\lambda_1) & -\frac{b-\lambda_1}{\lambda_1} \\ -(b-\lambda_2) & 1 & b-\lambda_2 & \frac{b-\lambda_2}{\lambda_2} \\ -b^2c & bc & 0 & -(b-\lambda_0)(b-\lambda_2)(b-\lambda_1) \end{pmatrix}$$

and scaling factors

$$\sigma_0 := \frac{\lambda_1 \lambda_2}{b(\lambda_0 - \lambda_2)(\lambda_0 - \lambda_1)}, \quad \sigma_1 := \frac{\lambda_0 \lambda_2}{b(\lambda_1 - \lambda_2)(\lambda_0 - \lambda_1)}, \quad \sigma_2 := \frac{\lambda_0 \lambda_1}{b(\lambda_1 - \lambda_2)(\lambda_0 - \lambda_2)}, \quad \sigma_3 := -\frac{1}{b^2 c}.$$

Thus, the solution of the initial value problem determined by (9) – (12) reads

$$z_1(y; s_1, s_2) = \sum_{k=0}^2 \frac{c - \lambda_k^2}{c} \sigma_k (-1)^k \left(s_1 + \frac{b - \lambda_k}{\lambda_k} s_2 \right) e^{\lambda_k y} - \sigma_3 \left(b^2 c T_b - b c s_1 + s_2 \prod_{k=0}^2 (b - \lambda_k) \right) \quad (23a)$$

$$z_2(y; s_1, s_2) = \sum_{k=0}^2 \frac{c - \lambda_k^2}{c} \lambda_k \sigma_k (-1)^k \left(s_1 + \frac{b - \lambda_k}{\lambda_k} s_2 \right) e^{\lambda_k y}, \quad (23b)$$

$$z_3(y; s_1, s_2) = \sum_{k=0}^2 \sigma_k (-1)^k \left(s_1 + \frac{b - \lambda_k}{\lambda_k} s_2 \right) e^{\lambda_k y} - \sigma_3 \left(b^2 c T_b - b c s_1 + s_2 \prod_{k=0}^2 (b - \lambda_k) \right), \quad (23c)$$

$$z_4(y; s_1, s_2) = \sum_{k=0}^2 \lambda_k \sigma_k (-1)^k \left(s_1 + \frac{b - \lambda_k}{\lambda_k} s_2 \right) e^{\lambda_k y}. \quad (23d)$$

The parameters (s_1, s_2) are now chosen such that the boundary conditions (13) hold at $y = L$ with $\mathbf{z}(L; s_1, s_2)$ determined by (23). This is equivalent to solving the linear 2×2 system

$$\mathbf{C} \mathbf{s} = \mathbf{b} \quad (24)$$

for $\mathbf{s} = (s_1, s_2)^T$ with matrix \mathbf{C} and right-hand side \mathbf{b} determined by

$$\mathbf{C} := \begin{pmatrix} \sum_{k=0}^2 (-1)^k \lambda_k^2 \frac{d_k^-}{d_k^+} e^{\lambda_k L} & \sum_{k=0}^2 (-1)^k \lambda_k d_k^- e^{\lambda_k L} \\ \sum_{k=0}^2 (-1)^k (a + b \lambda_k) d_k^- e^{\lambda_k L} & \sum_{k=0}^2 (-1)^k \frac{a + b \lambda_k}{\lambda_k} d_k^- d_k^+ e^{\lambda_k L} \end{pmatrix}, \quad \mathbf{b} := \begin{pmatrix} 0 \\ \gamma \frac{d_0^+ d_1^+ d_2^+ d_0^- d_1^- d_2^-}{b c} \end{pmatrix}$$

with

$$d_0^\pm := \lambda_1 \pm \lambda_2, \quad d_1^\pm := \lambda_0 \pm \lambda_2, \quad d_2^\pm := \lambda_0 \pm \lambda_1. \quad (25)$$

Note that by means of (18) it holds

$$d_k^+ = b - \lambda_k = \frac{a \lambda_k}{c - \lambda_k^2}, \quad k = 0, 1, 2, \quad (26)$$

$$d_0^+ d_1^+ d_2^+ = -b a, \quad (27)$$

$$d_0^- d_1^- d_2^- = -\frac{c d_k^-}{\lambda_k \sigma_k}. \quad (28)$$

Hence, the right-hand side of (24) simplifies to $\mathbf{b} = (0, -\gamma a d_0^- d_1^- d_2^- / c)^T$. Assuming that $\mathbf{C}^0 := (\mathbf{c}_1, \mathbf{c}_2)$ is a regular matrix, the parameters (s_1, s_2) are determined by

$$s_1 = \frac{\det(\mathbf{C}^1)}{\det(\mathbf{C}^0)} = \frac{c_{22} b_1 - c_{12} b_2}{c_{11} c_{22} - c_{21} c_{12}}, \quad \mathbf{C}^1 := (\mathbf{b}, \mathbf{c}_2), \quad (29a)$$

$$s_2 = \frac{\det(\mathbf{C}^2)}{\det(\mathbf{C}^0)} = \frac{c_{11} b_2 - c_{21} b_1}{c_{11} c_{22} - c_{21} c_{12}}, \quad \mathbf{C}^2 := (\mathbf{c}_1, \mathbf{b}) \quad (29b)$$

with

$$\det(\mathbf{C}^0) = \sum_{j,k=0}^2 C_{k,j}^0 e^{\lambda_k L} e^{\lambda_j L}, C_{k,j}^0 := (-1)^{k+j} (a + b \lambda_j) \frac{\lambda_k d_j^- d_k^-}{\lambda_j d_k^+} (\lambda_k d_j^+ - \lambda_j d_k^+) \quad (30a)$$

$$\det(\mathbf{C}^1) = \sum_{k=0}^2 c_k^1 e^{\lambda_k L}, c_k^1 := -\gamma \frac{d_0^+ d_1^+ d_2^+ d_0^- d_1^- d_2^-}{bc} (-1)^k \lambda_k d_k^- = (-1)^k \frac{\gamma a}{c} d_0^- d_1^- d_2^- \lambda_k d_k^-, \quad (30b)$$

$$\det(\mathbf{C}^2) = \sum_{k=0}^2 c_k^2 e^{\lambda_k L}, c_k^2 := \gamma \frac{d_0^+ d_1^+ d_2^+ d_0^- d_1^- d_2^-}{bc} (-1)^k \lambda_k^2 \frac{d_k^-}{d_k^+} = -(-1)^k \frac{\gamma a}{c} d_0^- d_1^- d_2^- \lambda_k^2 \frac{d_k^-}{d_k^+}. \quad (30c)$$

Computing the parameters s_1 and s_2 using the formulae (29) and (30) is not feasible because $a, b \gg 1$ and, thus, the positive eigenvalues are large, i.e., $\lambda_0, \lambda_2 \gg 1$. For a stable evaluation, it is recommended to factorize the largest exponential term, $\exp((\lambda_0 + \lambda_2)L)$, from the determinants. For this purpose, we first note that the number of summands in the determinant of the matrix \mathbf{C}^0 can be reduced employing symmetry in the coefficients

$$\overline{C}_{kj}^0 := C_{kj}^0 + C_{jk}^0 = (-1)^{k+j+1} \frac{d_0^- d_1^- d_2^-}{ac} (a(a + \lambda_j \lambda_k) + b^2 c) d_i^+ d_i^- \quad (31)$$

for $k, i, j \in \{0, 1, 2\}$, $k < j$ and $i \neq k, j$. In particular, we make use of the relations (18) and (15). Factorizing the largest exponential term from the determinants yields

$$\det(\mathbf{C}^0) = e^{(\lambda_0 + \lambda_2)L} (\overline{C}_{02}^0 + c_R^0), \det(\mathbf{C}^1) = e^{(\lambda_0 + \lambda_2)L} c_R^1, \det(\mathbf{C}^2) = e^{(\lambda_0 + \lambda_2)L} c_R^2 \quad (32)$$

with coefficients

$$c_R^0 := (\overline{C}_{01}^0 e^{(\lambda_1 - \lambda_2)L} + \overline{C}_{12}^0 e^{(\lambda_1 - \lambda_0)L}), \quad (33a)$$

$$c_R^1 := (c_0^1 e^{-\lambda_2 L} + c_1^1 e^{(\lambda_1 - \lambda_0 - \lambda_2)L} + c_2^1 e^{-\lambda_0 L}), \quad (33b)$$

$$c_R^2 := (c_0^2 e^{-\lambda_2 L} + c_1^2 e^{(\lambda_1 - \lambda_0 - \lambda_2)L} + c_2^2 e^{-\lambda_0 L}). \quad (33c)$$

Finally, we can rewrite the parameters s_1 and s_2 as

$$s_1 = \frac{c_R^1}{\overline{C}_{02}^0 + c_R^0}, \quad s_2 = \frac{c_R^2}{\overline{C}_{02}^0 + c_R^0}. \quad (34)$$

So far we assume regularity and, thus, the existence of the parameters (s_1, s_2) . We now verify regularity of the matrix \mathbf{C}^0 .

Lemma 1 (Regularity of matrix \mathbf{C}^0).

The determinant of the matrix \mathbf{C}^0 is positive, i.e., \mathbf{C}^0 is regular, for all $L \geq 0$. In particular, the linear system of equations (24) has a unique solution determined by (29) or, equivalently, (34).

Proof. According to (32), (31) and (33a), the determinant of the matrix \mathbf{C}^0 can be written as

$$\det(\mathbf{C}^0) = -e^{(\lambda_0 + \lambda_2)L} \frac{d_0^- d_1^- d_2^-}{ac} \left(\overline{C}_{02}^0 + \overline{C}_{01}^0 e^{(\lambda_1 - \lambda_2)L} + \overline{C}_{12}^0 e^{(\lambda_1 - \lambda_0)L} \right) \quad (35)$$

with coefficients

$$\overline{C}_{kj}^0 := -\frac{ac}{d_0^- d_1^- d_2^-} \overline{C}_{kj}^0 = (-1)^{k+j} (a(a + \lambda_j \lambda_k) + b^2 c) d_i^+ d_i^-, \quad i, k, j \in \{0, 1, 2\}, \quad k \neq j \neq i. \quad (36)$$

To estimate the sign of the determinant, we will employ the following estimates

$$d_0^- = \lambda_1 - \lambda_2 < 0, \quad d_1^- = \lambda_0 - \lambda_2 > 0, \quad d_2^- = \lambda_0 - \lambda_1 > 0, \quad (37a)$$

$$d_0^+ = \lambda_1 + \lambda_2 < 0, \quad d_1^+ = \lambda_0 + \lambda_2 > 0, \quad d_2^+ = \lambda_0 + \lambda_1 > 0, \quad (37b)$$

$$\lambda_0 > 0, \quad \lambda_1 < 0, \quad \lambda_2 > 0 \quad (37c)$$

that hold because of Proposition 1. Then the prefactor in (35) is positive. Obviously, the coefficient \overline{C}_{02}^0 is also positive. To determine the sign of the determinant, we now distinguish four cases for the the sign of the remaining two coefficients to estimate the sum in the parentheses.

Case 1: If both \overline{C}_{01}^0 and \overline{C}_{12}^0 are positive, then all the terms in the parentheses of (35) are positive.

Case 2: If both \overline{C}_{01}^0 and \overline{C}_{12}^0 are negative, then we deduce by means of (37)

$$\overline{C}_{02}^0 + \overline{C}_{01}^0 e^{(\lambda_1 - \lambda_2)L} + \overline{C}_{12}^0 e^{(\lambda_1 - \lambda_0)L} \geq \overline{C}_{02}^0 + \overline{C}_{01}^0 + \overline{C}_{12}^0 = -ab d_0^- d_1^- d_2^- > 0.$$

Case 3: If \overline{C}_{01}^0 is positive and \overline{C}_{12}^0 is negative, then the following estimate holds

$$\overline{C}_{02}^0 + e^{(\lambda_1 - \lambda_2)L} \left(\overline{C}_{01}^0 + \overline{C}_{12}^0 e^{(\lambda_2 - \lambda_0)L} \right) \geq e^{(\lambda_1 - \lambda_2)L} \left(\overline{C}_{02}^0 + \overline{C}_{01}^0 + \overline{C}_{12}^0 \right) \geq 0.$$

Case 4: Finally, assuming that \overline{C}_{01}^0 is negative and \overline{C}_{12}^0 is positive, the definition (36) of the coefficients implies $\lambda_2 > \lambda_0$. This contradicts (37a). Thus, this case cannot occur.

Finally, we conclude that the determinant of the matrix \mathbf{C}^0 is positive for all $L > 0$. \square

Since now the parameters can be computed, we consider next the evaluation of the temperatures $T_f(y) \equiv z_1(y; s_1, s_2)$ and $T_s(y) \equiv z_3(y; s_1, s_2)$. Again, the formulae (23a) and (23c) are not feasible because of the large exponential factors. Therefore, we proceed as before and factorize the largest factor, where we split $T_{f,s}$ in a non-constant and a constant part. We do this separately for the terms

$$T_{f,s}(y) = \overline{T}_{f,s}(y) + \overline{T} := \sum_{k=0}^2 c_{f,s}^k b_k e^{\lambda_k y} - \sigma_3 \left(c b^2 T_b - c b s_1 + s_2 \prod_{k=0}^2 (b - \lambda_k) \right), \quad (38a)$$

$$c_f^k := (-1)^k \frac{\sigma_k c - \lambda_k^2}{\lambda_k c}, \quad c_s^k := (-1)^k \frac{\sigma_k}{\lambda_k}, \quad b_k := \lambda_k s_1 + (b - \lambda_k) s_2. \quad (38b)$$

Inserting (34) into the term \overline{T} and employing the splitting $\overline{C}_{02}^k + c_R^k$ into large and small contributions, we obtain a similar splitting

$$\overline{T} := \frac{1}{1 + \overline{c}_R^0} (\overline{T}_1 + \overline{T}_2),$$

$$\overline{T}_1 := -\sigma_3 b^2 c T_b = T_b,$$

$$\overline{T}_2 := -\sigma_3 \frac{1}{\overline{C}_{02}^0} (b^2 c T_b c_R^0 - b c c_R^1 + c_R^2 (b - \lambda_0)(b - \lambda_1)(b - \lambda_2))$$

$$= \overline{T}_{01} e^{(\lambda_1 - \lambda_2)L} + \overline{T}_{12} e^{(\lambda_1 - \lambda_0)L} + \overline{T}_0 e^{-\lambda_2 L} + \overline{T}_1 e^{(\lambda_1 - \lambda_0 - \lambda_2)L} + \overline{T}_2 e^{-\lambda_0 L},$$

$$\overline{T}_{kj} := -\sigma_3 \frac{\overline{C}_{kj}^0}{\overline{C}_{02}^0} b^2 c T_b = \frac{\overline{C}_{kj}^0}{\overline{C}_{02}^0} T_b = (-1)^{k+j} \frac{d_i^- d_i^+}{d_1^- d_1^+} \frac{a(a + \lambda_j \lambda_k) + b^2 c}{a(a + \lambda_0 \lambda_2) + b^2 c} T_b,$$

$$\overline{T}_k := \sigma_3 \frac{1}{\overline{C}_{02}^0} (b c c_k^1 - (b - \lambda_0)(b - \lambda_1)(b - \lambda_2) c_k^2) = (-1)^k \frac{\gamma a^2}{c b} \frac{1}{a(a + \lambda_0 \lambda_2) + c b^2} \frac{d_k^- \lambda_k^3}{d_1^- d_1^+},$$

$$\overline{c}_R^0 := \frac{c_R^0}{\overline{C}_{02}^0} = \overline{c}_{01}^0 e^{(\lambda_1 - \lambda_2)L} + \overline{c}_{12}^0 e^{(\lambda_1 - \lambda_0)L},$$

$$\overline{c}_{kj}^0 := \frac{\overline{C}_{kj}^0}{\overline{C}_{02}^0} = (-1)^{k+j} \frac{d_i^- d_i^+}{d_1^- d_1^+} \frac{a(a + \lambda_j \lambda_k) + b^2 c}{a(a + \lambda_0 \lambda_2) + b^2 c} = \frac{\overline{T}_{kj}}{T_b}.$$

Next we consider $\bar{T}_{f,s}$. We start with separating small and large contributions in the coefficients b_k :

$$\begin{aligned} b_k &:= \frac{b_k^2}{1 + \bar{c}_R^0}, \\ b_k^2 &:= \frac{1}{\bar{C}_{02}^0} (\lambda_k c_R^1 + (b - \lambda_k) c_R^2) = \bar{b}_k^0 e^{-\lambda_2 L} + \bar{b}_k^1 e^{(\lambda_1 - \lambda_0 - \lambda_2)L} + \bar{b}_k^2 e^{-\lambda_0 L}, \\ \bar{b}_k^l &:= \frac{1}{\bar{C}_{02}^0} (\lambda_k c_l^1 + (b - \lambda_k) c_l^2) = (-1)^l \frac{\gamma b a^2}{a(a + \lambda_0 \lambda_2) + c b^2} \frac{1}{d_1^- d_1^+} \frac{\lambda_l d_l^-}{d_l^+} (\lambda_l - \lambda_k). \end{aligned}$$

Incorporating the splitting of b_k in $\bar{T}_{f,s}$, we obtain

$$\begin{aligned} \bar{T}_{f,s}(y) &:= \frac{1}{1 + \bar{c}_R^0} \bar{T}_{f,s}^2(y), \\ \bar{T}_{f,s}^2(y) &:= \sum_{k=0}^2 c_{f,s}^k b_k^2 e^{\lambda_k y} = \sum_{k=0}^2 \bar{T}_{f,s}^{2,k}(y), \\ \bar{T}_{f,s}^{2,0}(y) &:= \sum_{k=0}^2 c_{f,s}^k \bar{b}_k^0 e^{-\lambda_2 L + \lambda_k y} = \sum_{k=1,2} c_{f,s}^k \bar{b}_k^0 e^{-\lambda_2 L + \lambda_k y} = \sum_{k=1,2} \bar{c}_{f,s}^{0,k} e^{-\lambda_2 L + \lambda_k y}, \\ \bar{T}_{f,s}^{2,1}(y) &:= \sum_{k=0}^2 c_{f,s}^k \bar{b}_k^1 e^{(\lambda_1 - \lambda_0 - \lambda_2)L + \lambda_k y} = \sum_{k=0,2} c_{f,s}^k \bar{b}_k^1 e^{(\lambda_1 - \lambda_0 - \lambda_2)L + \lambda_k y} = \sum_{k=0,2} \bar{c}_{f,s}^{1,k} e^{(\lambda_1 - \lambda_0 - \lambda_2)L + \lambda_k y}, \\ \bar{T}_{f,s}^{2,2}(y) &:= \sum_{k=0}^2 c_{f,s}^k \bar{b}_k^2 e^{-\lambda_0 L + \lambda_k y} = \sum_{k=0,1} c_{f,s}^k \bar{b}_k^2 e^{-\lambda_0 L + \lambda_k y} = \sum_{k=0,1} \bar{c}_{f,s}^{2,k} e^{-\lambda_0 L + \lambda_k y}, \\ \bar{c}_f^{l,k} &:= c_f^k \bar{b}_k^l = (-1)^{l+k+1} \frac{\gamma b a^2}{a(a + \lambda_0 \lambda_2) + c b^2} \frac{1}{d_0^- d_1^- d_2^-} \frac{1}{d_1^+ d_1^+} \frac{d_l^- d_k^-}{d_l^+} \frac{\lambda_l}{\lambda_k^2} (c - \lambda_k^2) (\lambda_l - \lambda_k), \\ \bar{c}_s^{l,k} &:= c_s^k \bar{b}_k^l = (-1)^{l+k+1} \frac{\gamma b a^2}{a(a + \lambda_0 \lambda_2) + c b^2} \frac{1}{d_0^- d_1^- d_2^-} \frac{1}{d_1^+ d_1^+} \frac{\lambda_l}{\lambda_k} \frac{d_k^- d_l^-}{d_l^+} c (\lambda_l - \lambda_k). \end{aligned}$$

Combining the above formulae, we obtain the following representation for the temperatures

$$\begin{aligned} T_{f,s}(y) = T_b - \frac{\gamma a d_0^- d_1^- d_2^-}{c \bar{C}_{02}^0 + c_R^0} &\left(\bar{c}_{f,s}^{0,1} e^{-\lambda_2 L + \lambda_1 y} + \bar{c}_{f,s}^{0,2} e^{-\lambda_2 L + \lambda_2 y} + \bar{c}_{f,s}^{1,0} e^{(\lambda_1 - \lambda_0 - \lambda_2)L + \lambda_0 y} + \right. \\ &\bar{c}_{f,s}^{1,2} e^{(\lambda_1 - \lambda_0 - \lambda_2)L + \lambda_2 y} + \bar{c}_{f,s}^{2,0} e^{-\lambda_0 L + \lambda_0 y} + \bar{c}_{f,s}^{2,1} e^{-\lambda_0 L + \lambda_1 y} + \\ &\left. \frac{1}{c b} \left(\bar{\bar{T}}_0 e^{-\lambda_2 L} + \bar{\bar{T}}_1 e^{(\lambda_1 - \lambda_0 - \lambda_2)L} + \bar{\bar{T}}_2 e^{-\lambda_0 L} \right) \right) \end{aligned} \quad (39)$$

with coefficients for $l, k, i \in \{0, 1, 2\}$, $l \neq k \neq i$,

$$\bar{c}_f^{l,k} := -\frac{c}{\gamma a} \bar{C}_{02}^0 \frac{1}{d_0^- d_1^- d_2^-} \bar{c}_f^{l,k} = (-1)^{l+k} \text{sign}(k - l) \frac{d_i^+ \lambda_l}{\lambda_k}, \quad (40a)$$

$$\bar{c}_s^{l,k} := -\frac{c}{\gamma a} \bar{C}_{02}^0 \frac{1}{d_0^- d_1^- d_2^-} \bar{c}_s^{l,k} = (-1)^{l+k} \text{sign}(k - l) \frac{\lambda_i \lambda_l^2}{\lambda_k d_l^+}, \quad (40b)$$

$$\bar{\bar{T}}_k := -\frac{c}{\gamma b a} \bar{C}_{02}^0 \frac{c b^2}{d_0^- d_1^- d_2^-} \bar{\bar{T}}_k = (-1)^k \lambda_k^3 d_k^- \quad (40c)$$

and \bar{C}_{02}^0 , c_R^0 , d_k^\pm defined by (33a), (31) and (25), respectively. Furthermore, the parameters a , b , c and γ are defined in (11) and (14b). Finally, the eigenvalues λ_k are determined by (16).

To derive properties of the solution of the boundary value problem (9) – (13), the monotonicity of the temperatures is of key importance. For this purpose, we consider the derivative of the temperatures given by

$$T'_{f,s}(y) = -\frac{\gamma a d_0^- d_1^- d_2^-}{c \overline{C}_{02}^0 + c_R^0} \left(\overline{d}_{f,s}^{0,1} e^{-\lambda_2 L + \lambda_1 y} + \overline{d}_{f,s}^{0,2} e^{-\lambda_2 L + \lambda_2 y} + \overline{d}_{f,s}^{1,0} e^{(\lambda_1 - \lambda_0 - \lambda_2)L + \lambda_0 y} + \overline{d}_{f,s}^{1,2} e^{(\lambda_1 - \lambda_0 - \lambda_2)L + \lambda_2 y} + \overline{d}_{f,s}^{2,0} e^{-\lambda_0 L + \lambda_0 y} + \overline{d}_{f,s}^{2,1} e^{-\lambda_0 L + \lambda_1 y} \right) \quad (41)$$

with coefficients $\overline{d}_{f,s}^{l,k} := \overline{c}_{f,s}^{l,k} \lambda_k$.

Lemma 2 (Estimates for the derivatives of the temperatures).

Let be $L > 0$. Then the derivatives of the temperatures can be estimated by

$$T'_f(y) \geq \frac{\gamma a (d_0^- d_1^- d_2^-)^2}{c^2 \overline{C}_{02}^0 + c_R^0} e^{-\lambda_2 L + \lambda_2 y} \geq 0, \quad T'_s(y) \geq \frac{\gamma a (d_0^- d_1^- d_2^-)^2}{c^2 \overline{C}_{02}^0 + c_R^0} e^{(\lambda_1 - \lambda_0 - \lambda_2)L + \lambda_2 y} \geq 0 \quad (42)$$

for $0 \leq y \leq L$. In particular, the derivatives vanish if and only if $\gamma = 0$.

Proof. Since by Lemma 1 the determinant of the matrix \mathbf{C}^0 is positive, the term $\overline{C}_{02}^0 + c_R^0$ is positive as well. By means of the estimates (37), the prefactor in (41) is positive and it holds

$$\begin{aligned} \overline{d}_f^{0,1} < 0, \quad \overline{d}_f^{0,2} > 0, \quad \overline{d}_f^{1,0} < 0, \quad \overline{d}_f^{1,2} < 0, \quad \overline{d}_f^{2,0} < 0, \quad \overline{d}_f^{2,1} < 0, \\ \overline{d}_s^{0,1} > 0, \quad \overline{d}_s^{0,2} > 0, \quad \overline{d}_s^{1,0} > 0, \quad \overline{d}_s^{1,2} < 0, \quad \overline{d}_s^{2,0} > 0, \quad \overline{d}_s^{2,1} > 0. \end{aligned}$$

For the sum in the parenthesis in (41), we consider the fluid and the solid case separately. According to the eigenvalues, the term $e^{-\lambda_2 L + \lambda_2 y}$ decays much slower than the other exponential terms. For the fluid temperature, we factorize this term and estimate the remaining part by

$$\begin{aligned} & \overline{d}_{f,s}^{0,1} e^{(\lambda_1 - \lambda_2)y} + \overline{d}_{f,s}^{0,2} + \overline{d}_{f,s}^{1,0} e^{(\lambda_1 - \lambda_0)L + (\lambda_0 - \lambda_2)y} + \\ & \overline{d}_{f,s}^{1,2} e^{(\lambda_1 - \lambda_0)L} + \overline{d}_{f,s}^{2,0} e^{(\lambda_2 - \lambda_0)(L-y)} + \overline{d}_{f,s}^{2,1} e^{(\lambda_2 - \lambda_0)L + (\lambda_1 - \lambda_2)y} \geq \\ & \overline{d}_f^{0,1} + \overline{d}_f^{0,2} + \overline{d}_f^{1,0} + \overline{d}_f^{1,2} + \overline{d}_f^{2,0} + \overline{d}_f^{2,1} = \frac{d_0^- d_1^- d_2^- (\lambda_0 + \lambda_1 + \lambda_2)}{\lambda_0 \lambda_1 \lambda_2} = -\frac{d_0^- d_1^- d_2^-}{c}. \end{aligned}$$

Here we use that for $0 \leq y \leq L$ all exponents are non-positive and, thus, the exponential functions can be estimated by 1 from above, whereas the factors of these exponential terms are all negative.

For the solid temperature, we proceed similarly. According to the eigenvalues, the term $e^{(\lambda_1 - \lambda_0 - \lambda_2)L + \lambda_2 y}$ decays much faster than the other exponential terms. Again, we factorize this term from the parenthesis term in (41) and estimate the remaining part by

$$\begin{aligned} & \overline{d}_{f,s}^{0,1} e^{(\lambda_0 - \lambda_1)L + (\lambda_1 - \lambda_2)y} + \overline{d}_{f,s}^{0,2} e^{(\lambda_0 - \lambda_1)L} + \overline{d}_{f,s}^{1,0} e^{(\lambda_0 - \lambda_2)L} + \\ & \overline{d}_{f,s}^{1,2} + \overline{d}_{f,s}^{2,0} e^{(\lambda_2 - \lambda_1)L + (\lambda_0 - \lambda_2)y} + \overline{d}_{f,s}^{2,1} e^{(\lambda_2 - \lambda_1)(L-y)} \geq \\ & \overline{d}_s^{0,1} + \overline{d}_s^{0,2} + \overline{d}_s^{1,0} + \overline{d}_s^{1,2} + \overline{d}_s^{2,0} + \overline{d}_s^{2,1} = \frac{d_0^- d_1^- d_2^- (\lambda_0 + \lambda_1 + \lambda_2)}{\lambda_0 \lambda_1 \lambda_2} = -\frac{d_0^- d_1^- d_2^-}{c}. \end{aligned}$$

Here we use that for $0 \leq y \leq L$ all exponents are non-negative and, thus, the exponential functions can be estimated by 1 from below, whereas the factors of these exponential terms are all positive.

Finally, combining the above findings we conclude with the estimates (42). Note that equality only holds if $\gamma = 0$. \square

Next we investigate the temperature difference $T_s - T_f$ that according to (39) is given by

$$T_s(y) - T_f(y) = -\frac{\gamma a}{c} \frac{d_0^- d_1^- d_2^-}{\overline{C}_{02}^0 + c_R^0} \left(\check{c}^{0,1} e^{-\lambda_2 L + \lambda_1 y} + \check{c}^{0,2} e^{-\lambda_2 L + \lambda_2 y} + \check{c}^{1,0} e^{(\lambda_1 - \lambda_0 - \lambda_2)L + \lambda_0 y} + \check{c}^{1,2} e^{(\lambda_1 - \lambda_0 - \lambda_2)L + \lambda_2 y} + \check{c}^{2,0} e^{-\lambda_0 L + \lambda_0 y} + \check{c}^{2,1} e^{-\lambda_0 L + \lambda_1 y} \right) \quad (43)$$

with coefficients

$$\check{c}^{l,k} := \overline{c}_s^{l,k} - \overline{c}_f^{l,k} = (-1)^{l+k} \text{sign}(k-l) \frac{\lambda_l}{\lambda_k d_l^+} (\lambda_i \lambda_l - d_i^+ d_l^+) = (-1)^{l+k+1} \text{sign}(k-l) \frac{\lambda_l b}{d_l^+} \quad (44a)$$

for $l, k, i \in \{0, 1, 2\}$, $l \neq k \neq i$.

Lemma 3 (Estimates of the temperature difference).

Let be $L > 0$. Then the difference of the temperatures can be estimated by

$$T_s(y) \geq T_f(y), \quad y \in [0, L]. \quad (45)$$

In particular, the temperatures coincide if and only if $\gamma = 0$.

Proof. Since by Lemma 1 the determinant of the matrix \mathbf{C}^0 is positive, the term $\overline{C}_{02}^0 + c_R^0$ is positive as well. By means of the estimates (37), the prefactor in (43) is positive and it holds

$$\check{c}^{0,2} = -\check{c}^{0,1} > 0, \quad \check{c}^{1,0} = -\check{c}^{1,2} > 0, \quad \check{c}^{2,0} = -\check{c}^{2,1} > 0.$$

Then the sum in the parenthesis of (43) can be estimated by

$$\begin{aligned} & \check{c}^{0,2} (e^{-\lambda_2 L + \lambda_2 y} - e^{-\lambda_2 L + \lambda_1 y}) + \check{c}^{1,0} (e^{(\lambda_1 - \lambda_0 - \lambda_2)L + \lambda_0 y} - e^{(\lambda_1 - \lambda_0 - \lambda_2)L + \lambda_2 y}) + \\ & \check{c}^{2,0} (e^{-\lambda_0 L + \lambda_0 y} - e^{-\lambda_0 L + \lambda_1 y}) \geq 0, \end{aligned}$$

where we employ positivity of the coefficients and (37a). Finally, combining the above findings we conclude with the estimate (45). Note that due to (43) equality only holds if $\gamma = 0$. \square

By means of Lemma 1, 2 and 3, we may now conclude on the following properties of the temperatures.

Proposition 2 (Properties of the temperature system with fluid heat conduction).

The following properties hold true for the temperature system determined by the boundary value problem (9) – (13) and arbitrary $0 < L < \infty$:

(i) There exists a unique solution of the boundary value problem (9) – (13) determined by (23) with (s_1, s_2) the solution of (24).

(ii) If $\gamma > 0$, i.e.,

$$q_{HG} > 0, \quad (46)$$

then it holds:

(1) The temperature difference $T_s - T_f$ is positive.

(2) The coolant temperature T_f is monotonically increasing and

$$T_f(y) \geq T_b, \quad y \in [0, L]. \quad (47)$$

(3) The solid temperature T_s is monotonically increasing and

$$T_s(y) \geq T_b, \quad y \in [0, L]. \quad (48)$$

(iii) If $\gamma = 0$, i.e., $q_{HG} = 0$, then the temperatures are constant and it holds:

$$T_f(y) = T_s(y) = T_b, \quad y \in [0, L]. \quad (49)$$

Proof. The existence of a unique solution is ensured by the regularity of the matrix \mathbf{C}^0 according to Lemma 1 providing us with unique parameters (s_1, s_2) determined by (34).

For $\gamma > 0$, we conclude by Lemma 2 that the temperatures T_f and T_s are strictly monotonically increasing and, thus, by the initial conditions (12) are larger than or equal to T_b . Furthermore, Lemma 3 verifies that T_s is always larger than or equal to T_f .

Finally, for $\gamma = 0$, we conclude from (39) that both temperatures coincide with the initial value T_b . \square

Remark 3 (Simplified temperature system). *In [9], Appendix A, the solution to the simplified temperature system determined by (6) and corresponding boundary conditions (4a), (4b) at $y = 0$ and (5c) at $y = L$ is determined as*

$$T_f(y) = T_b - \bar{r} \bar{a} \frac{\lambda_- - \lambda_+ + \lambda_+ e^{\lambda_- y} - \lambda_- e^{\lambda_+ y}}{\lambda_+^2 e^{\lambda_- L} - \lambda_-^2 e^{\lambda_+ L}}, \quad (50a)$$

$$T_s(y) = T_b + \bar{r} \frac{\lambda_+^2 e^{\lambda_- y} - \lambda_-^2 e^{\lambda_+ y} - (\lambda_- - \lambda_+) \bar{a}}{\lambda_+^2 e^{\lambda_- L} - \lambda_-^2 e^{\lambda_+ L}} \quad (50b)$$

with

$$\bar{a} := \frac{h_v A_c}{c_{p,f} \dot{m}_c}, \quad \bar{b} := \frac{h_v}{(1 - \varphi) \kappa_s}, \quad (51)$$

$$\lambda_{\pm} = \frac{1}{2} \left(-\bar{a} \pm \sqrt{\bar{a}^2 + 4\bar{b}} \right), \quad (52)$$

$$\bar{r} := \frac{\bar{a}}{h_v} q_{HG}. \quad (53)$$

For these temperatures, the same properties hold true as in Proposition 2.

4 Mass-momentum system

For the investigation of the mass-momentum system determined by (2) and corresponding initial values (5a) and (5b), it is useful to rewrite the model in a more canonical form. Employing constant mass flow (1) and conservation of mass, the mass-momentum equations (2a) and (2b) can be rewritten and we finally obtain the system of ordinary differential equations (ODEs)

$$\rho_f'(y) = \bar{N}((\rho_f, v, T_f, T_s)(y)) \rho_f(y), \quad (54a)$$

$$v'(y) = -\bar{N}((\rho_f, v, T_f, T_s)(y)) v(y) \quad (54b)$$

for $y \in (0, L)$ with initial values

$$\rho_f(L) = \frac{p_{HG}}{R T_f(L)}, \quad (55a)$$

$$v(L) = \frac{\dot{m}_c R T_f(L)}{A_c p_{HG}} \quad (55b)$$

and coefficient

$$\bar{N}(\rho_f, v, T_f, T_s) := \frac{R(c_{p,f} \dot{m}_c)^{-1} h_v A_c \rho_f (T_s - T_f) + K_D^{-1} \mu_f v + K_F^{-1} \rho_f v^2}{\rho_f (\varphi^{-2} v^2 - R T_f)}. \quad (56)$$

By means of the mass conservation (1), we can substitute the velocity by the density in (56). Since we already know the temperatures, the coefficient \bar{N} becomes a function that only depends on the density and the position, whereas the temperatures enter as parameters:

$$\bar{N}(y, \rho_f; T_f, T_s) = \frac{R(c_{p,f} \dot{m}_c)^{-1} h_v A_c \rho_f^2(y) (T_s(y) - T_f(y)) + \dot{m}_c A_c^{-1} (K_D^{-1} \mu_f + K_F^{-1} \dot{m}_c A_c^{-1})}{\varphi^{-2} (\dot{m}_c A_c^{-1})^2 - R T_f(y) \rho_f^2(y)}. \quad (57)$$

We then solve the backward initial value problem

$$\rho_f'(y) = \overline{N}(y, \rho_f; T_f, T_s) \rho_f(y), \quad y \in (0, L), \quad (58a)$$

$$\rho_f(L) = \frac{p_{HG}}{RT_f(L)} \quad (58b)$$

with an ODE solver from top ($y = L$) to bottom ($y = 0$). Note that $T_f(L)$ can be computed from (50a) and p_{HG} is assumed to be given. If this initial value problem has a unique solution, we may determine the reservoir pressure p_R by

$$p_R = \rho_f(0) RT_b. \quad (59)$$

The solution to the initial value problem (58) is not known explicitly. However, it can be verified that for arbitrary $L > 0$ there exists a unique solution provided that the heat flux at the interface is positive, i.e., (46) holds, and

$$\rho_f(L) > \sqrt{\frac{\varphi^{-2}(\dot{m}_c A_c^{-1})^2}{RT_b}} = \frac{\dot{m}_c}{\varphi A_c} \frac{1}{\sqrt{RT_b}}. \quad (60)$$

Proposition 3 (Existence and uniqueness of the density).

Let T_f, T_s be the unique solution of the temperature system (9) – (13) determined by (39). Let the data q_{HG} and p_{HG} be chosen such that (46) and (60) hold. Then the initial value problem (58) has a unique solution in $[0, L]$ for arbitrary $L > 0$. In particular, the density is positive and strictly monotonically decreasing.

Proof. First of all, we perform the change of coordinates $\bar{y}(y) := L - y$, $y \in [0, L]$, and the change of variables $\bar{\rho}(\bar{y}) := \rho(y(\bar{y}))$ to rewrite (58) as forward problem:

$$\bar{\rho}'(\bar{y}) = \overline{\overline{N}}(\bar{y}, \bar{\rho}_f; \overline{T}_f, \overline{T}_s) \bar{\rho}_f(\bar{y}) =: \bar{f}(\bar{y}, \bar{\rho}_f(\bar{y})), \quad \bar{y} \in (0, L), \quad (61a)$$

$$\bar{\rho}_f(0) = \frac{p_{HG}}{RT_f(L)} =: \bar{\rho}_0, \quad (61b)$$

where $\overline{\overline{N}}(\bar{y}, \bar{\rho}_f; \overline{T}_f, \overline{T}_s) := \overline{N}(y(\bar{y}), \rho_f; T_f, T_s)$ and $\overline{T}_f(\bar{y}) := T_f(y(\bar{y}))$, $\overline{T}_s(\bar{y}) := T_s(y(\bar{y}))$. Since T_f and T_s are solutions of the initial value problem (9) satisfying in particular (6a) and (3a), it holds

$$\overline{T}'_f(\bar{y}) = \frac{h_v A_c}{c_{p,f} \dot{m}_c} (\overline{T}_f(\bar{y}) - \overline{T}_s(\bar{y})) = \frac{h_v A_c}{c_{p,f} \dot{m}_c} (T_f(y(\bar{y})) - T_s(y(\bar{y}))) = -T'_f(y(\bar{y})) \leq 0. \quad (62)$$

Here non-negativity is ensured by Proposition 2 because of assumption (46). We now rewrite $\overline{\overline{N}}$ as

$$\overline{\overline{N}}(\bar{y}, \bar{\rho}_f; \overline{T}_f, \overline{T}_s) = \frac{\dot{m}_c A_c^{-1} (K_D^{-1} \mu_f + K_F^{-1} \dot{m}_c A_c^{-1}) - R \overline{T}'_f(\bar{y}) \bar{\rho}_f^2(\bar{y})}{R \overline{T}_f(\bar{y}) \bar{\rho}_f^2(\bar{y}) - \varphi^{-2}(\dot{m}_c A_c^{-1})^2} =: \frac{\overline{Z}(\bar{y})}{\overline{D}(\bar{y})}.$$

Note that rewriting the initial value problem as forward problem is essential because data are given at $y = L$ rather than $y = 0$.

To verify the unique existence of the solution to (61), we proceed now similarly to the proof of the local Picard-Lindelöf theorem using the contraction mapping theorem. We recall this proof here because for our problem at hand we may exploit some problem-inherent properties, e.g., monotonicity. Repeated application of the local Picard-Lindelöf theorem will finally lead to a global result. We will proceed in three steps.

Step 1. First of all, we remind that the space $C([0, L])$ of continuous functions on $[0, L]$ equipped with the supremum norm is a Banach space. For a subspace, we consider the set $B_r([0, L]) := \{\bar{\rho} \in C([0, L]) : \bar{\rho}_0 \leq \bar{\rho}(\bar{y}) \leq \bar{\rho}_0 + r, \bar{y} \in [0, L]\}$ for some $r > 0$. Since $T_f \in C^1([0, L])$ and is positive, see Proposition 2, there exist bounds $0 = T'_m < T'_M$ such that $T'_m \leq -\overline{T}'_f(\bar{y}) = T'_f(y(\bar{y})) \leq T'_M$ for $\bar{y} \in [0, L]$. Furthermore, the temperature is bounded by $T_b \leq \overline{T}_f(\bar{y}) = T_f(y(\bar{y})) \leq T_f(L)$ due to monotonicity of T_f . Note that $T'_M = 0$

and $T_f(L) = T_b$ if “=” holds in (46). Then we may estimate the numerator \bar{Z} and the denominator \bar{D} for arbitrary $\bar{\rho} \in B_r([0, L])$ by

$$\begin{aligned}\bar{Z}_m(\bar{\rho}_0, r) &:= RT'_m \bar{\rho}_0^2 + \beta \leq \bar{Z}(\bar{y}) \leq RT'_M(\bar{\rho}_0 + r)^2 + \beta =: \bar{Z}_M(\bar{\rho}_0, r), \\ \bar{D}_m(\bar{\rho}_0, r) &:= RT_b \bar{\rho}_0^2 - \gamma \leq \bar{D}(\bar{y}) \leq RT_f(L)(\bar{\rho}_0 + r)^2 - \gamma =: \bar{D}_M(\bar{\rho}_0, r)\end{aligned}\quad (63)$$

with $\beta := \dot{m}_c A_c^{-1} (K_D^{-1} \mu_f + K_F^{-1} \dot{m}_c A_c^{-1}) > 0$ and $\gamma := \varphi^{-2} (\dot{m}_c A_c^{-1})^2 > 0$. The numerator is always positive because $T'_m = 0$. By assumption (60), the lower bound of the denominator is also positive provided that

$$\bar{\rho}_0 \geq \bar{\rho}(0) = \frac{p_{\text{HG}}}{RT_f(L)}.\quad (64)$$

Thus, the right-hand side of the ODE (61a) is positive and can be estimated by

$$0 < \bar{f}(\bar{y}, \bar{\rho}) \leq (\bar{\rho}_0 + r) \frac{\bar{Z}_M(\bar{\rho}_0, r)}{\bar{D}_m(\bar{\rho}_0, r)} =: M(\bar{\rho}_0, r), \quad \bar{y} \in [0, L], \quad \bar{\rho} \in B_r([0, L]).$$

Since the denominator is bounded away from zero and $\bar{T}_f \in C^1([0, L])$, the function $\bar{f} : [0, L] \times B_r([0, L]) \rightarrow \mathbb{R}_+$ is continuous in both arguments and differentiable in the second argument. In particular, \bar{f} is Lipschitz-continuous in the second argument because by the mean value theorem we have

$$|\bar{f}(\bar{y}, \bar{\rho}) - \bar{f}(\bar{y}, \bar{\bar{\rho}})| \leq \sup_{s \in [0, 1]} \left\{ \left| \frac{\partial \bar{f}}{\partial \bar{\rho}}(\bar{y}, \bar{\rho} + s(\bar{\bar{\rho}} - \bar{\rho})) \right| \right\} |\bar{\rho} - \bar{\bar{\rho}}| \leq K(\bar{\rho}_0, r) |\bar{\rho} - \bar{\bar{\rho}}|$$

for all $\bar{\rho}, \bar{\bar{\rho}} \in [\bar{\rho}_0, \bar{\rho}_0 + r]$ and $\bar{y} \in [0, L]$. Note that $B_r([0, L])$ is a convex set. To determine $K(\bar{\rho}_0, r)$, we first determine the derivative

$$\frac{\partial \bar{f}}{\partial \bar{\rho}}(\bar{y}, \bar{\rho}) = \frac{\gamma \left(3R\bar{T}'_f(\bar{y}) \bar{\rho}^2 - \beta \right) - R\bar{T}_f(\bar{y}) \bar{\rho}^2 \left(R\bar{T}'_f(\bar{y}) \bar{\rho}^2 + \beta \right)}{\left(R\bar{T}_f(\bar{y}) \bar{\rho}^2 - \gamma \right)^2}.$$

This can be estimated by

$$\left| \frac{\partial \bar{f}}{\partial \bar{\rho}}(\bar{y}, \bar{\rho}) \right| \leq \frac{\gamma \left(3RT'_M(\bar{\rho}_0 + r)^2 + \beta \right) + RT_f(L)(\bar{\rho}_0 + r)^2 \bar{Z}_M(\bar{\rho}_0, r)}{\bar{D}_m(\bar{\rho}_0, r)^2} =: K(\bar{\rho}_0, r).$$

Step 2. Now we are ready to prove the local existence of a unique solution to the initial value problem (61) on $[\bar{y}_0, \bar{y}_0 + \delta_0] \subset [0, L]$ with $\bar{y}_0 := 0$ and $\delta_0 := \min(L, r/M(\bar{\rho}_0, r), 1/(K(\bar{\rho}_0, r) + \epsilon))$ for some $\epsilon > 0$ arbitrarily small but fixed. Note that the estimates in Step 1 also hold for the domain $[\bar{y}_0, \bar{y}_0 + \delta_0]$ instead of $[0, L]$. We now apply the contraction mapping theorem to the fixed point problem: find $\bar{\rho} \in B_r([\bar{y}_0, \bar{y}_0 + \delta_0])$ such that $\Phi(\bar{\rho}) = \bar{\rho}$, where the fixed point function $\Phi : B_r([\bar{y}_0, \bar{y}_0 + \delta_0]) \rightarrow C([\bar{y}_0, \bar{y}_0 + \delta_0])$ is defined by

$$\Phi(\bar{\rho})(\bar{y}) := \bar{\rho}_0 + \int_{\bar{y}_0}^{\bar{y}} \bar{f}(s, \bar{\rho}(s)) ds, \quad \bar{y} \in [\bar{y}_0, \bar{y}_0 + \delta_0].$$

First of all, we note that Φ maps $B_r([0, \delta_0])$ onto itself. Obviously, the primitive function of a continuous function is continuous. Since by assumption (60) the function $\bar{f}(\bar{y}, \bar{\rho})$ is positive and bounded by $M(\bar{\rho}_0, r)$ for any function $\bar{\rho} \in B_r([0, \delta_0])$, we may estimate for $\bar{y} \in [\bar{y}_0, \bar{y}_0 + \delta_0]$

$$\bar{\rho}_0 \leq \Phi(\bar{\rho})(\bar{y}) = \bar{\rho}_0 + \int_{\bar{y}_0}^{\bar{y}} \bar{f}(s, \bar{\rho}(s)) ds \leq \bar{\rho}_0 + \delta_0 M(\bar{\rho}_0, r) \leq \bar{\rho}_0 + r.$$

Next we show that Φ is a contractive mapping. For this purpose, we first note that

$$|\Phi(\bar{\rho})(\bar{y}) - \Phi(\bar{\bar{\rho}})(\bar{y})| \leq \int_{\bar{y}_0}^{\bar{y}} |\bar{f}(s, \bar{\rho}(s)) - \bar{f}(s, \bar{\bar{\rho}}(s))| ds \leq \frac{K(\bar{\rho}_0, r)}{K(\bar{\rho}_0, r) + \epsilon} \|\bar{\rho} - \bar{\bar{\rho}}\|_{C([\bar{y}_0, \bar{y}_0 + \delta_0])}$$

for $\bar{y} \in [\bar{y}_0, \bar{y}_0 + \delta_0]$ and, thus,

$$\|\Phi(\bar{\rho}) - \Phi(\bar{\rho})\|_{C([\bar{y}_0, \bar{y}_0 + \delta_0])} \leq \frac{K(\rho_0, r)}{K(\rho_0, r) + \varepsilon} \|\bar{\rho} - \bar{\rho}\|_{C([\bar{y}_0, \bar{y}_0 + \delta_0])}.$$

The contraction mapping theorem then ensures the unique existence of $\bar{\rho} \equiv \bar{\rho}(\cdot, [\bar{y}_0, \bar{y}_0 + \delta_0]) \in B_r([\bar{y}_0, \bar{y}_0 + \delta_0])$ solving the initial value problem (61) on $[\bar{y}_0, \bar{y}_0 + \delta_0]$. The positivity of \bar{f} on $[\bar{y}_0, \bar{y}_0 + \delta_0] \times B_r([\bar{y}_0, \bar{y}_0 + \delta_0])$ implies that the derivative of $\bar{\rho}$ is positive and, thus, the density $\bar{\rho}$ is strictly monotonically increasing. Furthermore, since the initial data are positive, i.e., $\bar{\rho}_0 > 0$, the density must be positive as well.

Step 3. In general, we will not find $r > 0$ such that $\delta_0 = L$. Therefore, we repeat the above local procedure where we replace $\bar{y}_0, \bar{\rho}_0, \delta_0$ by $\bar{y}_{i+1} := \bar{y}_i + \delta_i, \bar{\rho}_{i+1} := \bar{\rho}(\bar{y}_{i+1}; [\bar{y}_i, \bar{y}_{i+1}])$ and $\delta_{i+1} := \min(L - \bar{y}_{i+1}, r/M(\bar{\rho}_{i+1}, r), 1/(K(\bar{\rho}_{i+1}, r) + \epsilon))$ for $i \in \mathbb{N}_0$. Note that due to monotonicity of the solution $\bar{\rho}(\cdot; [\bar{y}_i, \bar{y}_{i+1}])$ it holds $\bar{\rho}_i \leq \bar{\rho}_{i+1} \leq \bar{\rho}_i + r$ and therefore $\rho_0 \leq \bar{\rho}_{i+1} \leq \bar{\rho}_0 + (i+1)r$. The crucial question is whether we can reach the point $\bar{y} = L$ after a *finite* number of iterations, i.e., does there exist $n \in \mathbb{N}_0$ such that $\sum_{i=0}^n \delta_i = L$.

First of all, we observe that $K(\bar{\rho}_i, r)$ is bounded away from zero. In particular, $K(\bar{\rho}, r)$ tends to the ratio $T_f(L) T'_M/T_b^2 > 0$ for $\bar{\rho} \rightarrow \infty$. Thus, for i sufficiently large $\delta_i < 1/K(\bar{\rho}_i, r)$. On the other hand, $M(\bar{\rho}, r)$ tends to infinity for $\bar{\rho} \rightarrow \infty$. Thus, it might happen that $\delta_i = r/M(\bar{\rho}_i, r)$ for $i \geq i_0$. We now have to verify that $\sum_{i \geq i_0} r/M(\bar{\rho}_i, r)$ diverges. For this purpose, we first note that the ratio $\bar{Z}_M(\bar{\rho}, r)/\bar{D}_m(\bar{\rho}, r)$ tends to the ratio T'_M/T_b for $\bar{\rho} \rightarrow \infty$. Thus, this ratio stays bounded for $\bar{\rho} \in [\bar{\rho}_0, \infty)$, i.e., there exist constants $0 < c_m \leq c_M < \infty$ such that $c_m \leq \bar{Z}_M(\bar{\rho}, r)/\bar{D}_m(\bar{\rho}, r) < c_M$ for $\bar{\rho} \in [\bar{\rho}_0, \infty)$. Then we can estimate

$$\sum_{i=i_0}^n \frac{r}{M(\bar{\rho}_i, r)} = \sum_{i=i_0}^n \frac{r}{\bar{\rho}_i + r} \frac{\bar{D}_m(\bar{\rho}_i, r)}{\bar{Z}_M(\bar{\rho}_i, r)} \geq \frac{1}{c_M} \sum_{i=i_0}^n \frac{r}{\bar{\rho}_i + r} \geq \frac{1}{c_M} \sum_{i=i_0}^n \frac{r}{\bar{\rho}_0 + (i+1)r}.$$

The right-hand side tends to infinity for $n \rightarrow \infty$ since the harmonic sum is diverging. Thus, $\sum_{i > i_0}^n \delta_i \geq L$ for n sufficiently large. This proves uniqueness and existence of the solution to problem (61) in $[0, L]$. Since by definition $\rho_f(y) = \bar{\rho}(\bar{y}(y)) \geq \bar{\rho}_0$ and $\rho'_f(y) = -\bar{\rho}'(\bar{y}(y))$, the problem (58) also has a unique solution that is positive and strictly monotonically decreasing. \square

Note that the assumption (60) is crucial for the proof to ensure that the coefficient \bar{N} determined by (57) is negative. In [9], we verify that (60) holds for our envisaged applications.

Remark 4 (Density with the simplified temperature system). *In case of the simplified temperature system neglecting fluid heat conduction determined by (6) and corresponding boundary conditions (4a), (4b) at $y = 0$ and (5c) at $y = L$, the mass-momentum system does not change. Nevertheless, since the temperatures (50) enter the mass-momentum system as parameters, they affect its solution. The proof of Proposition 3 employs the properties of the temperatures in Proposition 2 which are the same for the temperature system with fluid heat conduction and the simplified one without. Therefore, Proposition 3 holds true also in case of the simplified system as was originally presented in [9], Appendix B.*

Velocity. Finally, we can determine the velocity by means of the mass conservation (1):

$$v(y) = \frac{\dot{m}_c}{A_c \rho_f(y)}, \quad y \in [0, L]. \quad (65)$$

In particular, (5b) holds at $y = L$. By Proposition 2 and 3, we then can draw the following conclusion.

Proposition 4 (Properties of the velocity).

Let the assumptions of Proposition 3 hold. Then the velocity is positive and strictly monotonically increasing.

Proof. Since the density is positive and strictly monotonically decreasing, we conclude from (65) the assertion. \square

Pressure. By the ideal gas law $p = \rho_f R T_f$, the density ρ_f and the temperature T_f of the coolant are linked with the pressure. Thus, the pressure is positive. In particular, the pressure is strictly monotonically

decreasing for arbitrary $L > 0$ provided the heat flux at the interface is positive, i.e., (46) holds, and the condition (60) is satisfied. This immediately follows from the derivative

$$p'(y) = R \rho_f(y) \frac{T_f'(y) \varphi^{-2} (\dot{m}_c A_c^{-1})^2 + \dot{m}_c A_c^{-1} (K_D^{-1} \mu_f + K_F^{-1} \dot{m}_c A_c^{-1})}{\varphi^{-2} (\dot{m}_c A_c^{-1})^2 - R T_f(y) \rho_f^2(y)} \quad (66)$$

determined by (58a) and (3a) or (6a). Since the derivative of T_f is positive, the numerator is positive. On the other hand, the denominator is negative due to assumption (60) and $\rho_f(y) \geq \rho_f(L)$. Thus, the derivative of the pressure is negative, i.e., the pressure is strictly monotonically decreasing.

Summary. Let the data T_b , p_{HG} , q_{HG} be chosen such that the estimates

$$q_{\text{HG}} \geq 0, \quad (67a)$$

$$\frac{p_{\text{HG}}}{R T_f(L)} \equiv \rho_f(L) > \frac{\dot{m}_c}{\varphi A_c} \frac{1}{\sqrt{R T_b}} \quad (67b)$$

hold. Then, there exists a unique solution to the model consisting of the mass-momentum system (2) and either the temperature system with fluid heat conduction (3) or the simplified temperature system (6) satisfying the boundary conditions (4a), (4b) at $y = 0$ as well as (5c), (5d) (the latter only for the system with fluid heat conduction) at $y = L$, where the reservoir pressure p_R is determined by

$$p_R = \rho_f(0) R T_b. \quad (68)$$

In particular, the temperatures T_f and T_s are determined by (39) or (50). The density ρ_f is given by the solution of (58). Finally, the velocity v is determined by (65).

5 Numerical Investigations

In the following, we numerically investigate whether the use of the simplified temperature system in a coupled transpiration cooling simulation is justified. The usual assumption for neglecting fluid heat conduction is $\kappa_f \ll \kappa_s$. However, we also investigate a case for which this constraint is violated, namely $\kappa_f = \kappa_s$. We use two 2D test cases, whose parameters are summarized in Tab. 1, simulating cooling gas injection into a subsonic turbulent hot gas channel flow. The channel has a length of 1.32 m and a height

		2D test case 1	2D test case 2	
porous material				
length (in flow direction y)	L	0.015	0.01	m
porosity	φ	0.111	0.111	-
permeability coefficient	K_D	$3.57 \cdot 10^{-13}$	$3.57 \cdot 10^{-13}$	m^2
Forchheimer coefficient	K_F	$5.17 \cdot 10^{-8}$	$5.17 \cdot 10^{-8}$	m
thermal conductivity solid	κ_s	15.19	12.5	W/(m K)
volumetric heat transfer coeff.	h_v	10^6	10^6	W/(m^3 K)
cooling gas (air) conditions				
coolant mass flow rate	\dot{m}_c	1.91	6.557	g/s
blowing ratio	F	0.0053	0.0035	-
backside solid temperature	T_b	321.9	304.2	K
thermal conductivity	κ_f	{ 0.03, 15.19 }	{ 0.03, 12.5 }	W/(m K)
dynamic viscosity	μ_f	$2.1 \cdot 10^{-5}$	$2.1 \cdot 10^{-5}$	Pa s
specific heat capacity	$c_{p,f}$	1004.5	1004.5	J/(kg K)
hot gas (air) conditions				
inflow Mach number	$Ma_{\text{HG},\infty}$	0.3	0.3	-
inflow temperature	$T_{\text{HG},\infty}$	425	1,800	K
inflow pressure	$p_{\text{HG},\infty}$	95.2	1,000	kPa

Table 1: Parameters for the two test cases.

	model	fluid heat cond.	κ_f	boundary condition at $y = L$
1	assembled-1D	yes	$\kappa_f \ll \kappa_s$	$T_f'(L) = \frac{h_v A_c}{c_{p,f} \dot{m}_c} (T_s(L) - T_f(L)) \neq 0$
2	original-2D	yes	$\kappa_f \ll \kappa_s$	$\nabla T_f(x, L) \cdot \vec{n} = 0$
3	assembled-1D	yes	$\kappa_f = \kappa_s$	$T_f'(L) = \frac{h_v A_c}{c_{p,f} \dot{m}_c} (T_s(L) - T_f(L)) \neq 0$
4	original-2D	yes	$\kappa_f = \kappa_s$	$\nabla T_f(x, L) \cdot \vec{n} = 0$
5	assembled-1D	no	-	-

Table 2: Simulations performed for each test case.

of 0.06 m. The original porous medium has a square cross section with a side length of 0.061 m and a resulting area of $A_c = 0.003721 \text{ m}^2$. It is mounted to the lower channel wall at $x = 0.58 \text{ m}$. Its length in y -direction is $L = 0.015 \text{ m}$ for test case 1 and $L = 0.01 \text{ m}$ for test case 2. The first test case originates from [4], whereas the second one is motivated by the numerical study in [17]. Both test cases were also used in [9]. The main differences between the two test cases are in the inflow temperature and inflow pressure of the hot gas flow.

For both test cases, five simulations are carried out as listed in Tab. 2. The first four simulations take into account fluid heat conduction with different values for the thermal conductivity κ_f of the fluid and with different boundary conditions regarding the first-order derivative of the fluid temperature T_f at the interface $y = L$ as discussed in Sect. 2. The fifth simulation neglects fluid heat conduction and, hence, uses the simplified temperature system. Simulations 1, 3 and 5 are conducted with our assembled-1D model presented in [9], i.e., by solving 1D problems in the porous medium, assembling the 1D solutions to obtain a 2D solution and coupling the latter with the solution of a 2D hot gas flow solver [20]. In case of the vanishing fluid temperature gradient in y -direction (simulations 2 and 4), we do not have at hand an analytical solution for the 1D temperature system. Hence, we use our original-2D approach [3–6] applying the same hot gas flow solver but a 2D solver for the porous medium flow. The latter was implemented using the finite element library deal.II [21].

Details on the coupled solution procedure, the setup of the solvers, the computational meshes and mesh convergence can be found in [9]. For the adiabatic side walls of the porous medium, in 1D we apply the side wall modeling as proposed and discussed also in [9]. For both test cases, we perform six coupling steps: porous medium flow and hot gas flow solutions are computed six times each in an alternating fashion. After each run of a flow solver, the coupling conditions on the interface are updated. For the chosen test cases, six steps are sufficient for the flow values on the interface to be converged in both domains.

5.1 Test case 1

The fluid temperature distribution inside the porous medium is depicted in Fig. 2 for all five simulations of test case 1. The differences between the solutions are small. The largest visible deviation concerns simulation 4 for $\kappa_f = \kappa_s$ with vanishing fluid temperature gradient at $y = L$, see Fig. 2d, around the upper left corner. The largest difference related to all other simulations is measured directly at the corner point and refers to simulation 2. However, it is only 5.5 K which corresponds to 1.6 %.

The influence of the different fluid temperature solutions on the hot gas temperature on the interface, i.e., at the cooling gas injection, and further downstream at the lower channel wall is investigated in Fig. 3. The temperature curves for simulations 1, 2 and 5 are virtually the same. Simulations 3 and 4 for $\kappa_f = \kappa_s$ show minimal differences but only between $x = 0.58 \text{ m}$ and $x = 0.641 \text{ m}$, i.e., on the interface: the temperatures of simulation 3 are slightly higher and the temperatures of simulation 4 slightly lower than the ones of the three other cases. However, the differences are clearly negligible.

A similar behavior becomes apparent in Fig. 4a showing the temperature throughout the porous medium for $y \in [0, L]$ at fixed position $x = 0.61 \text{ m}$. While the fluid and solid temperature curves for simulations 1, 2 and 5 coincide, the ones for simulations 3 and 4 with large κ_f deviate. Again, the temperatures of simulation 3 are larger than those of simulations 1, 2 and 5, whereas simulation 4 leads to lower temperatures. The adiabatic boundary condition at the interface $y = L$, which is prescribed in simulations 2 and 4, is only reflected by simulation 4. As explained in Sect. 2, this is due to the strong coupling of the two temperature equations and fluid heat conduction being negligible in case of

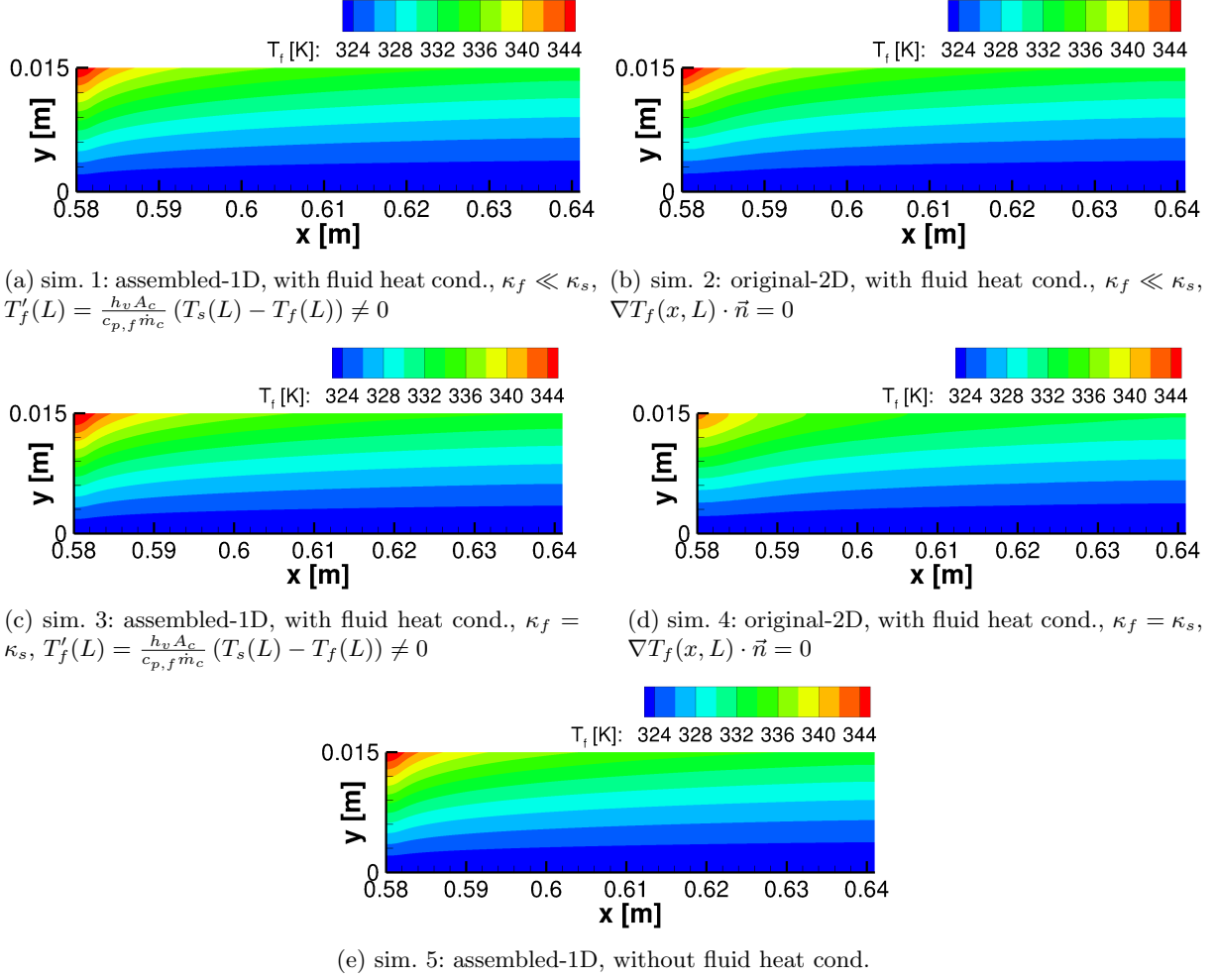


Figure 2: Test case 1: Fluid temperature T_f in the porous medium.

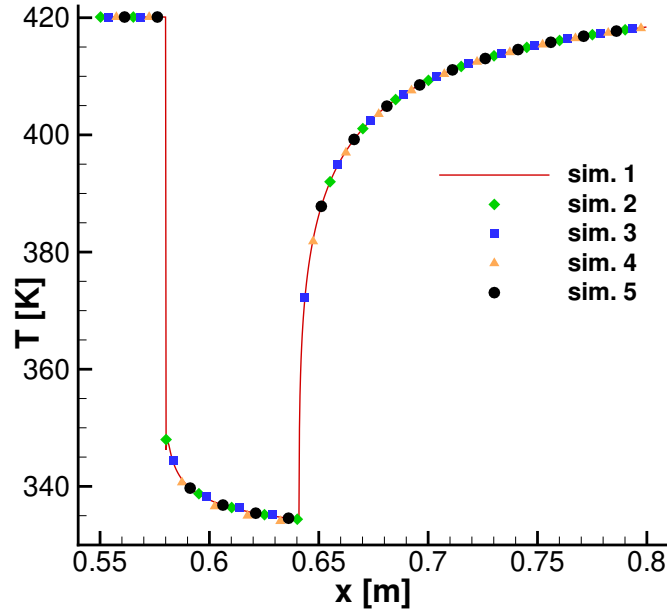


Figure 3: Test case 1: Lower wall hot gas temperature (cooling gas injection at $x \in [0.58, 0.641]$ m).

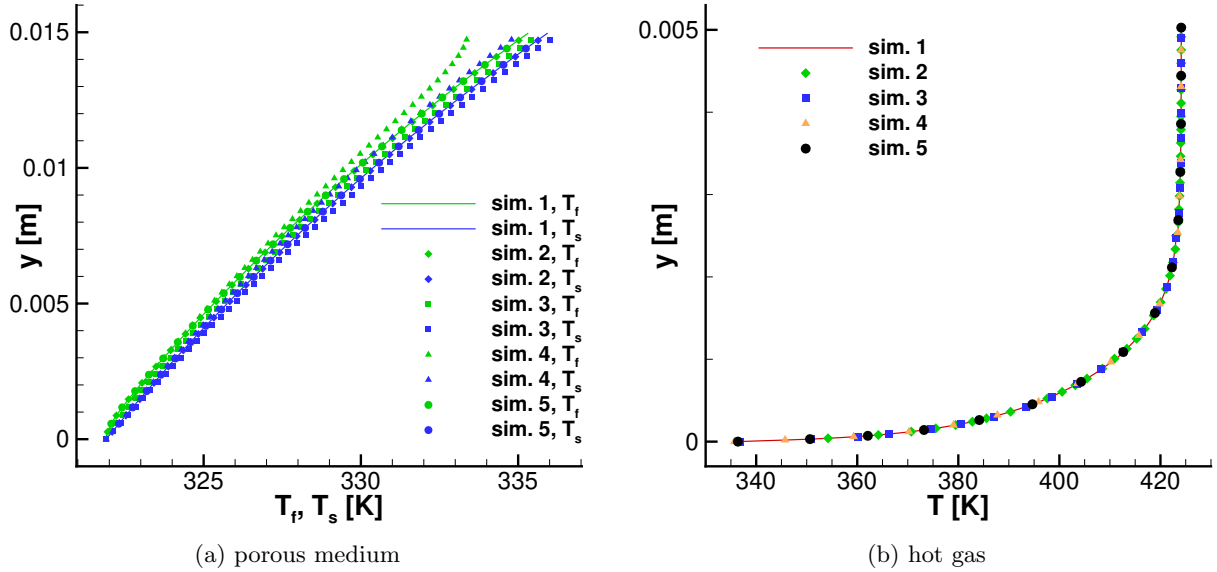


Figure 4: Test case 1: Temperatures at $x = 0.61$ m: (a) throughout the whole porous medium and (b) in the boundary layer of the hot gas flow.

simulation 2. The overall temperature behavior in the porous medium reveals that the choice of the boundary condition for $T'_f(L)$ in 1D or $\nabla T_f(x, L) \cdot \vec{n}$ in 2D/3D when taking into account fluid heat conduction has more influence than the choice whether to consider the latter at all. However, with maximum temperature differences of 2.1 K (0.6 %) and 1.2 K (0.4 %) for T_f and T_s , respectively, between simulations 3 and 4 at $y = L$, the influence on the cooling of the hot gas flow should be negligible. This is substantiated by Fig. 4b, depicting the hot gas temperature in the boundary layer at the same fixed position $x = 0.61$ m. All five curves are virtually the same with only minor differences in the initial temperature at $y = 0$ m due to the differences in the porous medium at $y = L$.

Since the differences in the fluid density ρ_f and the Darcy velocity v regarding the five simulations are analogously small and negligible, we do not present results for these two quantities.

5.2 Test case 2

Figures 5 to 7 show the results for the high-temperature test case 2 correspondingly to Figs. 2 to 4 of test case 1. The main results are analogous to those of test case 1. Again, the largest difference in the fluid temperatures in the porous medium concerns the upper left corner of simulations 2 and 4, cf. Fig. 5. At the corner point, the difference is 122.4 K which corresponds to 14.7 %. Even though this deviation is much larger than observed for test case 1 (1.6 %, see above), the influence on the hot gas flow again is small, see Fig. 6. This is due to the differences in the solutions being confined to a very small area around the upper left corner.

Figure 6 shows that, compared with test case 1, the larger differences in the porous medium temperatures lead to larger differences in the hot gas temperature at the injection. Again, the hot gas temperatures of simulation 3 are the highest and those of simulation 4 the lowest. However, the cooling effect on the lower channel wall downstream of the injection remains virtually the same for all five simulations.

The temperature curves in Fig. 7a first of all reveal a more pronounced temperature nonequilibrium than observed for test case 1, cf. Fig. 4a. Again, the differences in the temperature solutions are largest at the interface $y = L$. They amount to 45.8 K (7.3 %) and 24.1 K (3.2 %) for T_f and T_s , respectively, between simulations 3 and 4. Even though these deviations are significantly larger than those of test case 1 (0.6 % and 0.4 %, see above), the boundary layer temperature in the hot gas flow is virtually the same for all five simulations again as Fig. 7b reveals.

As the differences in the fluid density ρ_f and the Darcy velocity v are also small, we again omit presenting results for these two quantities.

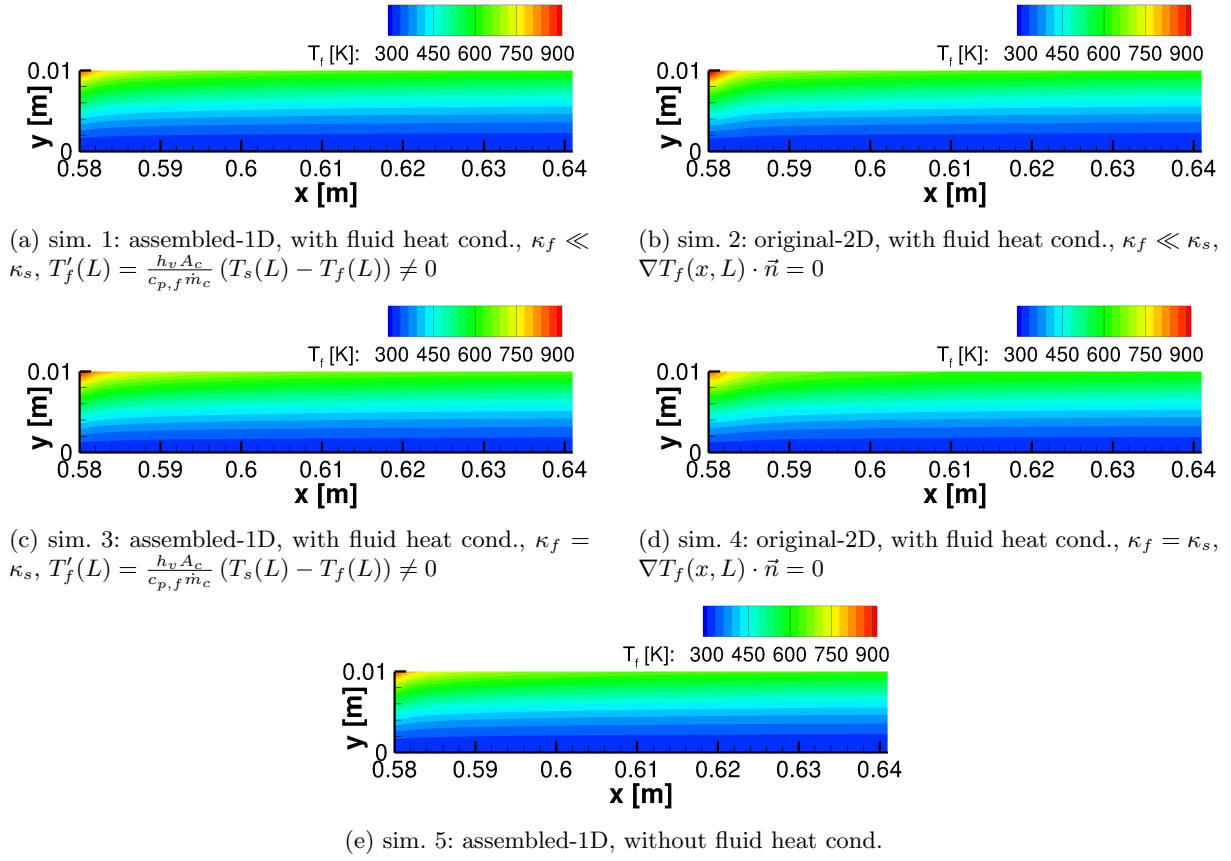


Figure 5: Test case 2: Fluid temperature T_f in the porous medium.

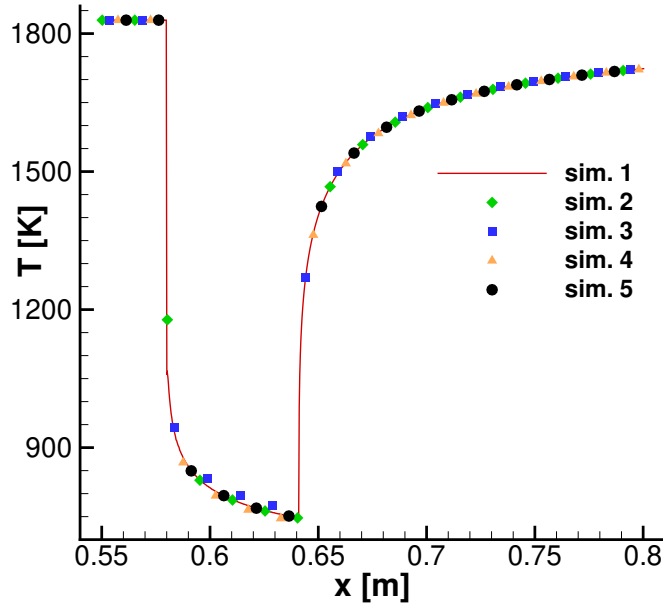


Figure 6: Test case 2: Lower wall hot gas temperature (cooling gas injection at $x \in [0.58, 0.641]$ m).

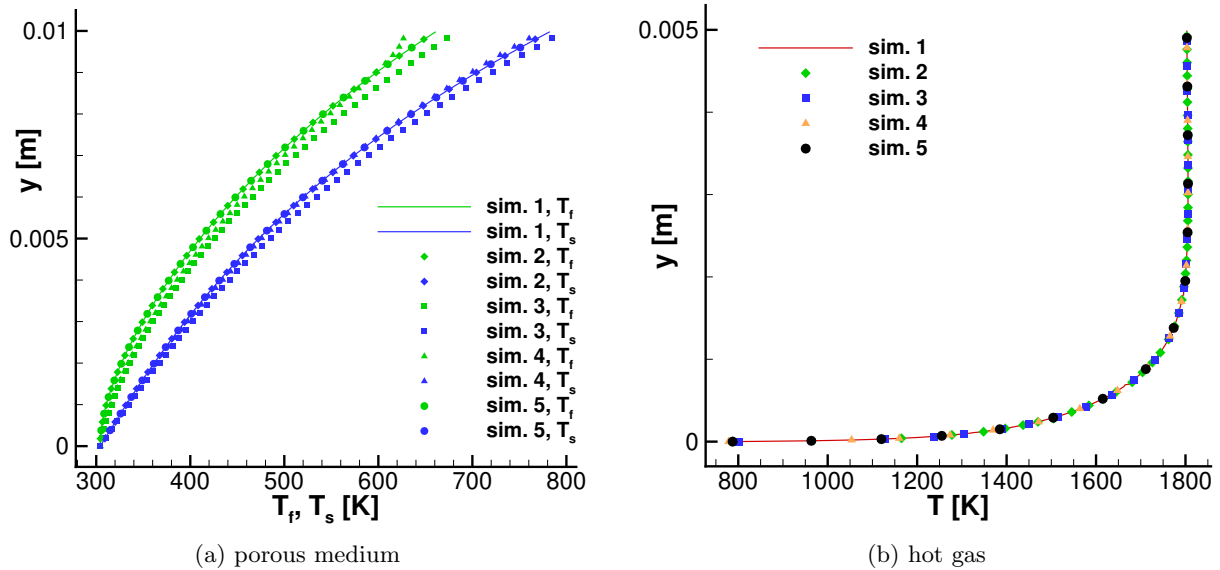


Figure 7: Test case 2: Temperatures at $x = 0.61$ m: (a) throughout the whole porous medium and (b) in the boundary layer of the hot gas flow.

6 Conclusion

A one-dimensional porous medium model for Darcy-Forchheimer flow under local thermal nonequilibrium has been investigated taking into account fluid heat conduction. This model consists of a linear temperature system for the fluid temperature and the solid temperature and a nonlinear mass-momentum system for the density of the fluid and the Darcy velocity. The temperature system is solved explicitly. Monotonicity properties of the temperature solution are employed to prove the existence of a unique solution to the mass-momentum system.

The 1D model is embedded in our assembled-1D model in [9] for the simulation of transpiration cooling problems, where a porous medium is mounted into a wall of a hot gas channel. Comparisons are performed with (i) solutions determined using a simplified 1D model omitting fluid heat conduction in the assembled-1D model and (ii) solutions using a full 2D porous medium model with different boundary conditions on the interface regarding fluid heat conduction. Computations are performed for two test cases with moderate and high temperatures in the hot gas channel. The numerical results show a very good agreement of the wall temperature in the hot gas both on top of the porous medium and downstream of the injection surface although there are some differences observable in the porous medium flow solutions near the injection surface. This also holds true if the fluid heat conduction is of the order of the solid heat conduction. This justifies the use of the simplified 1D porous medium model in our assembled-1D model for transpiration cooling.

References

- [1] E.R.G. Eckert, J.N.B. Livingood. Comparison of effectiveness of convection-, transpiration-, and film-cooling methods with air as coolant. National Advisory Committee for Aeronautics, Report 1182, 1954.
- [2] A.L. Laganelli. A comparison between film cooling and transpiration cooling systems in high speed flow. AIAA Paper No. 70-153, 1970.
- [3] W. Dahmen, T. Gotzen, S. Müller, M. Rom. Numerical simulation of transpiration cooling through porous material. International Journal for Numerical Methods in Fluids, 76 (6), 331-365, 2014.

- [4] W. Dahmen, S. Müller, M. Rom, S. Schweikert, M. Selzer, J. von Wolfersdorf. Numerical boundary layer investigations of transpiration-cooled turbulent channel flow. *International Journal of Heat and Mass Transfer*, 86, 90-100, 2015.
- [5] V. König, M. Rom, S. Müller, M. Selzer, J. von Wolfersdorf. Numerical and experimental investigation of transpiration cooling with carbon/carbon characteristic outflow distributions. *Journal of Thermophysics and Heat Transfer*, 33, 449-461, 2019.
- [6] V. König, M. Rom, S. Müller. A coupled two-domain approach for transpiration cooling. In: *Future Space-Transport-System Components under High Thermal and Mechanical Loads, Notes on Numerical Fluid Mechanics and Multidisciplinary Design 146*, N.A. Adams, W. Schröder, R. Radespiel, O.J. Haidn, T. Sattelmeyer, C. Stemmer, B. Weigand (eds.), Springer International Publishing, ISBN 978-3-030-53847-7, 2021.
- [7] W. Dahmen, V. Gerber, T. Gotzen, S. Müller, M. Rom, C. Windisch. Numerical simulation of transpiration cooling with a mixture of thermally perfect gases. In: *Proceedings of the Jointly Organized WCCM XI - ECCM V - ECFD VI 2014 Congress, Barcelona, Spain, 3012-3023*, 2014.
- [8] V. König, M. Rom, S. Müller. Influence of non-uniform injection into a transpiration-cooled turbulent channel flow: a numerical study. In: *2018 AIAA Aerospace Sciences Meeting, Kissimmee, Florida, AIAA 2018-0504*, 2018.
- [9] M. Rom, S. Müller. Derivation and analysis of a 1D porous medium flow solver embedded in a two-domain model for 2D and 3D transpiration cooling. *International Journal of Heat and Mass Transfer*, 195, 123127, 2022, DOI:10.1016/j.ijheatmasstransfer.2022.123127
- [10] H. Kubota. A simplified analytical solution for thermal response of a one-dimensional, steady state transpiration cooling system in radiative and convective environment. *NASA Technical Note D-8129*, 1976, <https://ntrs.nasa.gov/api/citations/19760007329/downloads/19760007329.pdf>
- [11] J. von Wolfersdorf. Effect of coolant side heat transfer on transpiration cooling. *Heat and Mass Transfer*, 41 (4), 327-337, 2005.
- [12] J.H. Wang, H.N. Wang. A discussion of transpiration cooling problems through an analytical solution of local thermal nonequilibrium model. *Journal of Heat Transfer*, 128 (10), 1093-1098, 2006.
- [13] J.H. Wang, J. Shi. Discussion of boundary conditions of transpiration cooling problems using analytical solution of LTNE model. *J. Heat Transfer*, 130 (1), 014504 (5 pages), 2008.
- [14] W. Zhang, Y. Yi, X. Bai, A. Nakayama. A local thermal non-equilibrium analysis for convective and radiative heat transfer in gaseous transpiration cooling through a porous wall. *International Journal of Heat and Mass Transfer*, 162, 120389, 2020.
- [15] X. Bai, Y. Yi, C. Liu, W. Zhang, A. Nakayama. A simple conjugate analysis and its comparison with experiment for heat transfer problems associated with hot gas flows in a partially transpiration-cooled channel. *International Journal of Heat and Mass Transfer*, 165, Part B, 120729, 2021.
- [16] A. Nakayama, Y. Yi, X. Bai, W. Zhang. A two-domain analytical approach for laminar and turbulent forced convection in a transpiration-cooled channel. *International Journal of Heat and Mass Transfer*, 184, 122247, 2022.
- [17] D.J. Munk, M. Selzer, G.P. Steven, G.A. Vio. Topology optimization applied to transpiration cooling. *AIAA Journal*, 57 (1), 297-312, 2019.
- [18] D. Prokein, C. Dittert, H. Böhrk, J. von Wolfersdorf. Numerical simulation of transpiration cooling experiments in supersonic flow using OpenFOAM. *CEAS Space Journal*, 12, 247-265, 2020.
- [19] R.S. Colladay, F.S. Stepka. Examination of boundary conditions for heat transfer through a porous wall. *NASA Technical Note D-6405*, 1971, <https://ntrs.nasa.gov/api/citations/19710020258/downloads/19710020258.pdf>

- [20] F. Bramkamp, P. Lamby, S. Müller. An adaptive multiscale finite volume solver for unsteady and steady state flow computations. *Journal of Computational Physics*, 197 (2), 460-490, 2004.
- [21] W. Bangerth, R. Hartmann, G. Kanschat. deal.II - a general-purpose object-oriented finite element library. *ACM Transactions on Mathematical Software*, 33 (4), 24/1-24/27, 2007.